International Journal of Research in Engineering and Science (IJRES)
ISSN (Online): 2320-9364, ISSN (Print): 2320-9356
www.ijres.org Volume 12 Issue 8 ǁ August 2024 ǁ PP. 89-114

An Experimental Investigation of Air Cooling for Photovoltaic Panels Using Air-Cooled Heat Sink: Case study Sfax-Tunisia

Mohamed Amine GHARBI[1]; Hichem ZAYANI[1,2]; Fedia MABROUK[1,3]; Said ZIANI[4,5]; Youssef AGREBI ZORGANI[1,2]

[1] Higher Institute of Technological Studies of Sfax, Route de Mahdia Km 2.5, 3099 El Bustan, Sfax, Tunisia
[2] Laboratory of Sciences and Techniques of Automatic Control and Computer Engineering (Lab-STA), National School of Engineering of Sfax, University of Sfax Postal Box 1173, 3038 Sfax, Tunisia
[3]Laboratory of Applied Fluid Mechanics, Process Engineering and Environment (Lab-MFAGPE), National School of Engineering of Sfax, University of Sfax Postal Box 1173, LR11ES57, 3038 Sfax, Tunisia.
[4]Laboratory of Networks, Computer Science, Telecommunication, Multimedia (RITM), Department of Electrical Engineering, High School of Technology ESTC, Hassan II University, Casablanca, Morocco.
*[5]Department of Health Technologies Engineering, Research Group in Biomedical Engineering and Pharmaceutical Sciences, ENSAM, Mohammed V University, Agdal, Morocco *1Department of Chemical*
Corresponding Author: mohamedamine.elgharbi@gmail.com; hichemzayani2@gmail.com; fedia_mabrouk@hotmail.fr; ziani9@yahoo.fr; agrebi69@yahoo.fr

Abstract
The objective of this paper is to design and implement a thermal photovoltaic sensor with energy recovery in order to improve the performance of the photovoltaic panel. Indeed, the temperature is a very important parameter in the behavior of solar cells; because the electrical performance of a solar cell is very sensitive to it. This study uses an experimental analysis to investigate the reduction in the operating temperature of PV panels with an air-cooled heat sink. The proposed heat sink was designed as a wood fins plate that is attached to the back of the PV panel. However, the influence of heat sinks on the heat transfer between a PV panel and the circulating ambient air was investigated and an experimental study to optimize the number of fins was carried out to ensure that the heat sink model worked properly. The results showed a substantial decrease in the operating temperature of the PV panel and an increase in its electrical performance as well as thermal gain was produced. As a consequence of decreasing its temperature, the heat sink increased the open-circuit photovoltage (V OC) and maximum power point (MPPT) of the PV panel. Therefore, the use of aluminum heat sinks could provide a potential solution to prevent PV panels from overheating and may indirectly lead to a reduction in CO2 emissions due to the increased electricity production from the PV system

Keywords: *Thermal photovoltaic sensor (PVT), solar radiation, fins, flow rate, electrical gain, thermal gain*.

Date of Submission: 09-08-2024 Date of acceptance: 21-08-2024

I. INTRODUCTION

Fossil fuels, such as natural gas, oil, nuclear energy, and coal, are the main sources of energy used by humanity. However, current stocks of fossil fuels are limited and not environmentally friendly. Fossil fuels emit many pollutants and cause serious environmental problems, such as global warming due to greenhouse gas emissions. They emit many pollutants and cause serious environmental problems, such as global warming due to greenhouse gas emissions.

Thus, renewable energy resources, which meet the criteria of green energy, are needed for global development and to meet the growing demand for energy worldwide. Solar energy, which is the main source of conventional and renewable energy, has great potential and a broad application of perspectives that can be used to meet most of the energy technology and photovoltaic technology, which can transform solar radiation into electrical energy thanks to photovoltaic panels [1].

Unfortunately for photovoltaic devices, at the current stage, only 20% of electromagnetic radiation is converted into electricity, while 80% is dissipated as heat causing an increase in the temperature of PV photovoltaic cells and which inevitably leads to a decline in its efficiency [2].

For this reason, comes the idea of combining the standard PV system with another thermal system to give a PVT thermal photovoltaic sensor which generates electricity in addition to heat. This system allows to recover the heat under the panels while ensuring a good thermal efficiency.

PVT thermal photovoltaic systems are very suitable alternatives not only to produce electricity but also can be used for drying all types of agricultural products, space heating and terrestrial applications. However,

Thermal photovoltaic solar hydride collectors (PV-T) have been studied and well developed during the last twenty years. Major research and development studies have been carried out on the recent technologies of hybrid modules (PV-T). Water solar hybrid systems (PV-T) are more efficient than air hybrid modules (PV-T) due to the good thermo-physical property of the first. However, experimental and numerical studies of hybrid air systems have been further developed, due to their relatively low construction cost and the operational costs of numerical simulations.

Most of the research in this area is aimed at optimizing the performance of existing solar components by improving operating conditions and subsequently evaluating the thermal and electrical performance of the module. In order to estimate their thermal and electrical performance Shan et al. [3], developed a series of mathematical models for five hybrid solar collectors (PV-T) to air that are differentiated by the cooling mode. Tonui and Tripanagnostopoulos [4], carried out experimental tests on three air-based solar collectors (PV-T) that operate in stable forced and natural state modes. The results of the latest authors have shown that the fin system is more suitable for air hybrid (PV-T) sensor systems, because the fin system has a much higher overall performance than the other two configurations. Othman et al [5] designed and built a prototype of a double-pass thermal photovoltaic solar collector, composed of parabolic concentrator (CPC) and fins. Dudul Das and all [6] and Ahmad Fudholi and all [7] have developed a digital model of a hybrid dual air solar collector (PV-T). The study shows that the expected results are in good agreement with the experimental results. Thus, the proposed mathematical model can be used to predict the temperatures of the different elements of the solar collector (PV-Th) with double air passage.

This paper is organized as follows. In the next section, the design of a thermal photovoltaic sensor (PVT) is introduced. The modeling of a photovoltaic panel is given in section 3. Furthermore, a simulation results are presented such as I-V and P-V characteristics. Section 4 is devoted to air PVT sensor components. In Section 5, experimental results are given in order to highlight the performance of the proposed thermal photovoltaic sensor (PVT). These experimental results are presented for many test cases in order to determine the electrical and thermal gain. Finally, some concluding remarks are given in section 6.

II. DESIGN OF A THERMAL PHOTOVOLTAIC SENSOR (PVT)

The high level of sunshine in Tunisia, especially in spring and summer, has a negative effect on photovoltaic cells and consequently on electricity efficiency. This requires action to reduce the surface temperature of the PV panel. Therefore, the electrical efficiency becomes more optimal and the collected thermal energy can be used in other applications. The thermal photovoltaic collector offers the possibility of producing hot air from solar radiation which is considered as the main and inexhaustible source in the planet.

The integration of PVT systems in buildings or in the agricultural sector offers savings on the heating bill and guarantees additional electricity production.

The proposed system consists of an ambient air ventilation system below the PV panel (Fig.1) aimed to absorb the heat recovered by the solar cells.

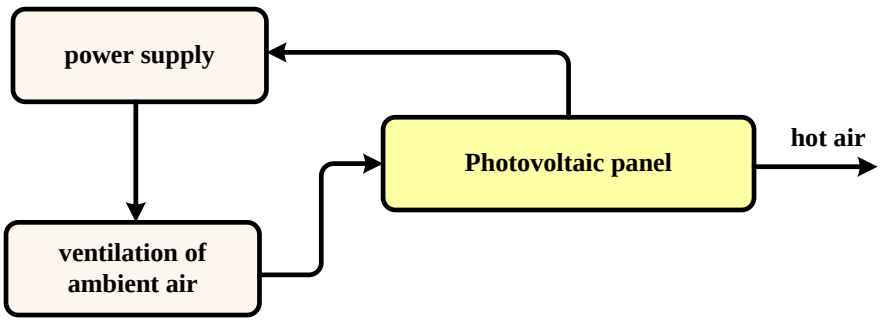

Figure 1. Synoptic of the solar panel cooling system

III. MODELING OF A PHOTOVOLTAIC PANEL

Solar cells are usually associated in series and in parallel, then encapsulated under glass to obtain a photovoltaic module. A PV generator is made up of modules interconnected to form a unit producing a high continuous power compatible with the usual electrical equipment. The interconnected modules are mounted on metal supports and inclined according to the desired angle depending on the location, this set is often designated as a module field. Thus, the characteristic I V of the PV generator is based on that of an elementary cell which is modelled by the equivalent circuit given in Figure 2.

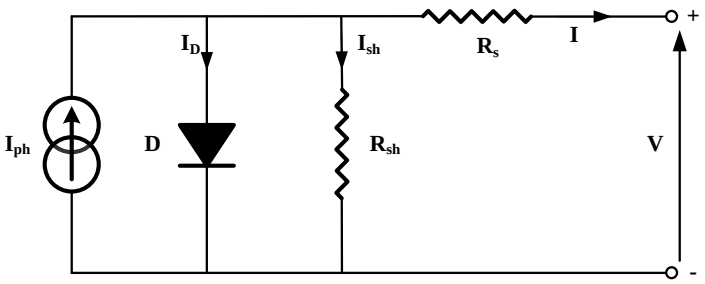

Figure 2. Equivalent circuit of a photovoltaic cell

This circuit can be used for both an elementary cell, a module or a panel consisting of several modules. The equation linking the current delivered by a PV module constituted by the series connection of Ns cells and the voltage at its terminals is given by:

$$\mathbf{I = I_{ph} - I_0 \cdot \left[exp\left(\frac{q\left(V + R_s \cdot I\right)}{n \cdot K \cdot N_s \cdot T} \right) - 1 \right] - I_{sh}} \quad (1)$$

Where: I_{ph}, I_0, n, q, K and T denote photocurrent, diode saturation current, diode ideality factor, electron charge, Boltzman constant, cell temperature which varies according to the illuminance and the ambient temperature.

The photo current I_{ph} is given by the following expression:

$$\mathbf{I_{ph} = \left[I_{sc} + k_i \cdot \left(T - 298 \right) \right] \cdot \frac{G}{1000}} \quad (2)$$

The diode saturation current is given by the equation below:

$$\mathbf{I_0 = I_{rs} \cdot \left(\frac{T}{T_n} \right)^3 \cdot exp\left[\frac{q \cdot E_{g0} \cdot \left(\frac{1}{T_n} - \frac{1}{T} \right)}{n \cdot K} \right]} \quad (3)$$

The reverse saturation current of the diode is given by equation 4:

$$\mathbf{I_{rs} = \frac{I_{sc}}{exp\left(\frac{q \cdot V_{oc}}{n \cdot N_s \cdot K \cdot T} \right) - 1}} \quad (4)$$

Equation 5 shows the expression for the current in the shunt resistor:

$$\mathbf{I_{sh} = \left(\frac{V + R_s \cdot I}{R_{sh}} \right)} \quad (5)$$

Hence the synoptic diagram of a photovoltaic cell is given by figure 3

The modeling of the photovoltaic panel, which is based on an algorithm developed from the physical equations, was tested by simulation with the Matlab- Simulink software.

The panel parameters are given by the table below:

Table 1 : **PV Panel Parameters**

Puissance nominale	275Wc
$\mathbf{V_{oc}}$: Tension en circuit ouvert (V)	38,05
$\mathbf{I_{sc}} = \mathbf{I_{cc}}$: Courant de court-circuit (A)	9,06
$\mathbf{N_s}$: Nombre total de cellules en série	60
$\mathbf{N_p}$: Nombre total de cellules en parallèle	1
$\mathbf{k_i}$: Courant de court-circuit de la cellule à 25°C et 1000 W/m^2	0,0032
T : Température de fonctionnement en K	T
$\mathbf{T_n}$: Température nominale en K	298
G : Rayonnement solaire (W/m^2)	G
q : Charge électronique (C)	1,6.10^{-19} C
n : Le facteur d'idéalité de la diode	1,3
K : Constante de Boltzmann (J/K)	1,38.10^{-23}
$\mathbf{E_{g0}}$: Energie de la largeur de bande du semiconducteur (eV)	1,1
$\mathbf{R_s}$: Resistance en série (Ω)	0,221
$\mathbf{R_{sh}}$: Resistance shunt (Ω)	415,405

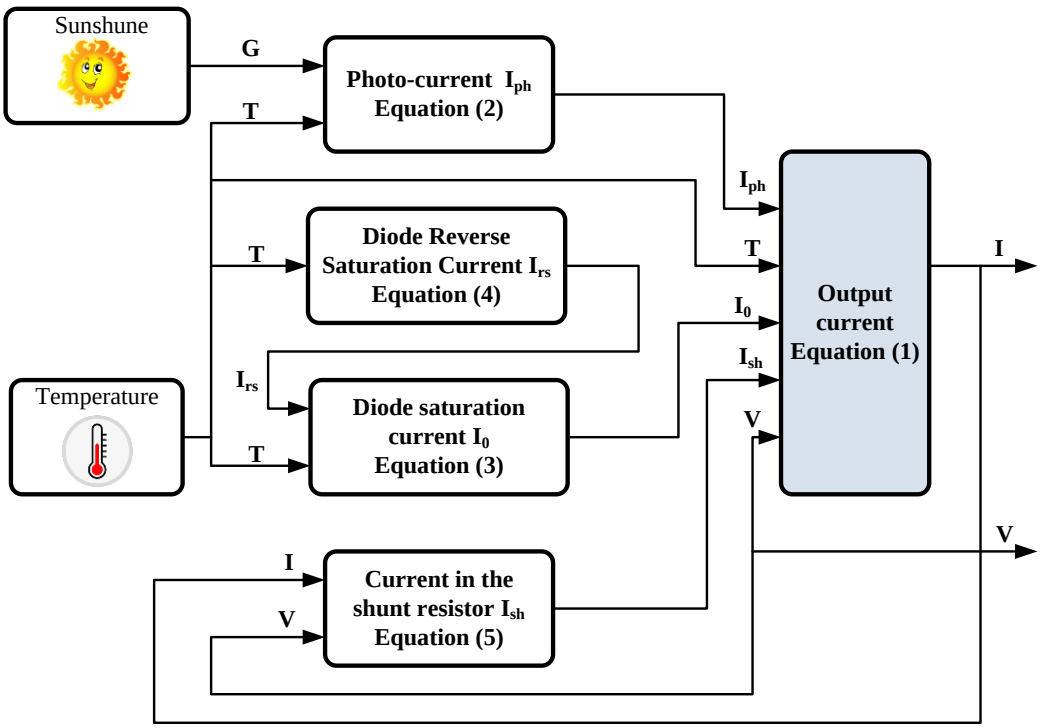

Figure 3. Synoptic diagram of a photovoltaic cell

To demonstrate the efficiency and performance of the proposed model, we test the system for the following modes of operation:

- Fixed temperature (28°C) and variable solar irradiation (625W/m^2 and 741W/m^2)
- Fixed solar irradiation (833W/m^2) and variable temperature (29°C and 33.1°C).

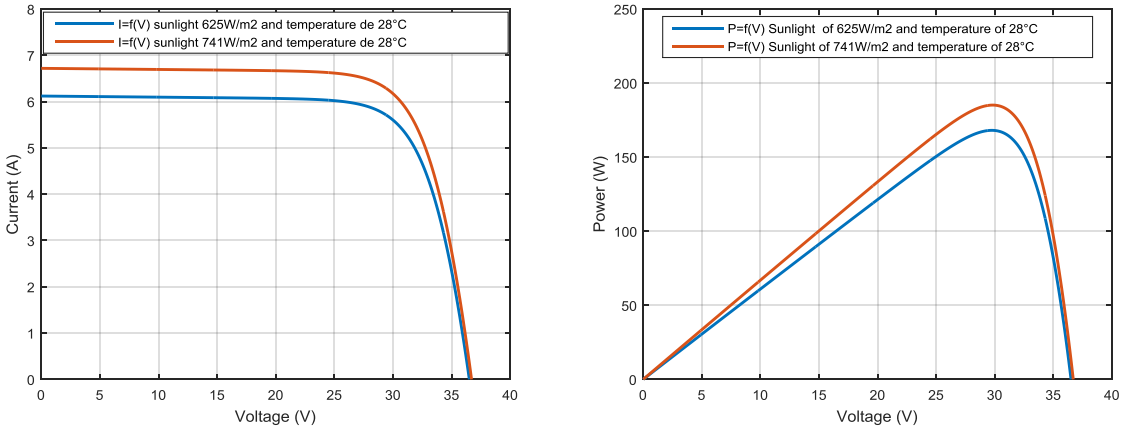

Figure 4. I-V and P-V characteristics of the module for different sunshine at T= Cte

When the solar radiation increases, the intensity of the photovoltaic current increases, the I −V curves (figure 4) shift towards increasing values allowing the module to produce a greater electrical power (figure 4). The current-voltage characteristic of the module shows a maximum power point with a voltage close to 30 Volts at 28°C and 741 W/m^2, according to the manufacturer's data. The photo-current is therefore directly linked to the luminous flux.

For fixed sunlight, the V_{OC} open circuit voltage increases with the decrease in temperature (Figure 5) while a small decrease is noted on the short circuit current I_{SC}=I_{CC}. The decrease in saturation current (I_O) is the main cause of the drop in current at low temperature.

Hence, for a PV generator to function optimally, on the one hand the temperature must be low and on the other hand the irradiance must be important.

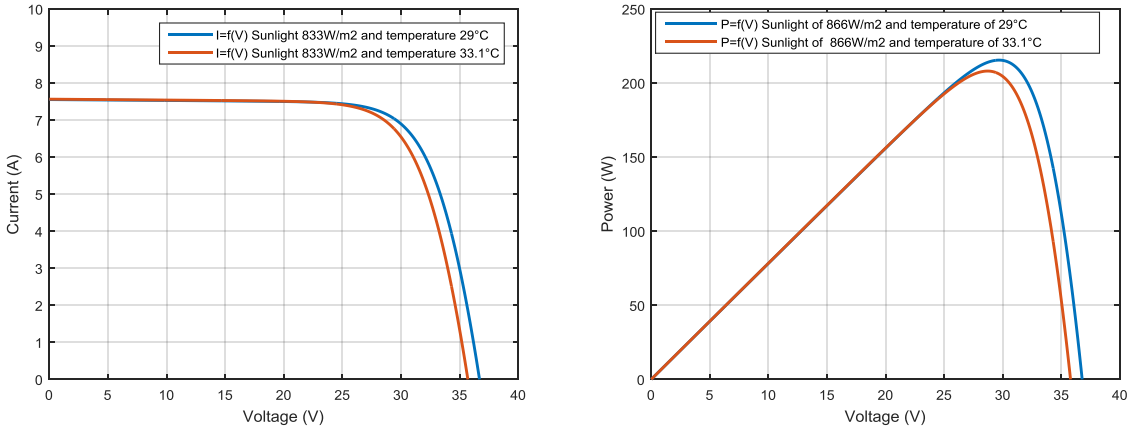

Figure 5: I-V and P-V characteristics of the module for different temperature at E=833W/m^2

IV. MODELING OF A PHOTOVOLTAIC PANEL

The installation of the prototype is located on the roof of the Sfax Higher Institute of Technological Studies (34.74°N, 10.76°E). We oriented the sensor in the south with an angle of inclination equal to 30°. The air PVT sensor is composed of two parts: a photovoltaic panel and an air thermal sensor. The essential elements of the thermal sensor are a metal plate, a funnel attached to the bottom of the panel and in which is placed the ventilator that will blow the air. The rear of the module is equipped with a set of obstacles or fins to slow down the thermo-circulation of the coolant in order to improve the thermal and electrical efficiency. Insulation is added on the back side of the metal plate and on the sides of the panel (Figure 6) to minimize heat loss.

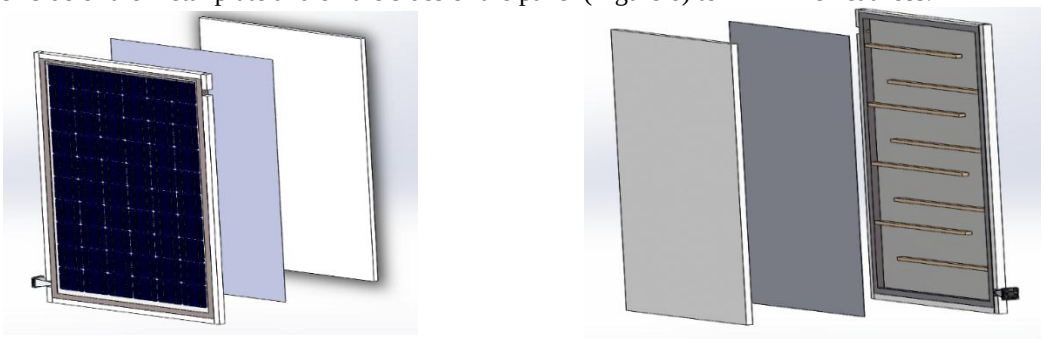

Figure 6. The essential elements and location of fins of the PVT thermal sensor

IV.1. The photovoltaic panel

The photovoltaic module is Soluxtec branded (see Appendix 1). It is a high quality and high-performance brand. Its dimensions are as follows:

Table 2: Dimension of the PV panel

Dimension of the PV panel	Length	Width	Thickness
	1645mm	985 mm	35 mm

The electrical characteristics of the module under STC conditions: (air mass AM 1.5, irradiation 1000W/m2, cell temperature 25°C) are as follows:

Tableau 3: Electrical characteristics of the PV panel

Maximum power (P max)	**275Wp**
Voltage at maximum power (Vmpp)	31,8 V
Current at maximum power (Impp)	8,65 A
Open circuit voltage (Voc)	38,05 V
Short circuit current (Icc ou Isc)	9,06 A

IV.2. The cooling fluid

The air circulation starts from the bottom through a small hole with a diameter of 18.5 mm reaching the top of the panel and exiting through a hole with the same diameter as that of the input. This circulation is ensured by means of a ventilator, which is provides a variable air flow by the speed variation which is controlled by a stabilized power supply (DC).

Taking into account the low heat capacity of the air (four times less than water), we have placed a set of fins to extend the residence time of the cold air to leave it the maximum time in contact with the hot side of the panel.

Table 4: Thermophysical properties of air

Physical properties	Symbols	Values
Volumic mass ($Kg.m^{-3}$)	P	1,22
Specific heat ($J.Kg^{-1}.K^{-1}$)	Cp	1012
Thermal conductivity ($J.m^{-1}.s^{-1}.K^{-1}$)	Λ	0.0242

IV.3. The metal supports

In the rear frame of the photovoltaic panel a galvanized steel plate with 1mm thick will be placed. The assembly of this plate is ensured by screws in order to be waterproof and easily removable.
The properties of galvanized steel are shown in the following table:

Table5: Thermo physical properties of metal plate

Physical properties	Symbols	Values
Density ($Kg.m^{-3}$)	P	7700
Specific heat (J.Kg1.K1)	Cp	435
Thermal conductivity ($J.m^{-1}.s^{-1}.K^{-1}$)	Λ	54
Melting temperature	T_{fusion}	1400-1500

IV.4. The fins

The rear frame of the photovoltaic panel is equipped with a set of obstacles or fins in wood of length 80cm, width 2 cm and thickness 3 cm. They are arranged in such a way as to slow down the circulation of air on the one hand and on the other hand will serve to increase its passage time so that it recovers more heat. However, in each time the number of baffles is varied to evaluate their influence on the thermal efficiency of the panel.

Table 6: Thermo physical properties of wood

Physical properties	Symbols	Values
Density ($Kg.m^{-3}$)	P	110-240
Specific heat (J.Kg1.K1)	Cp	2000-2 100
Thermal conductivity ($J.m^{-1}.s^{-1}.K^{-1}$)	Λ	0,038 - 0,049

IV.5. Thermal insulation

In order to limit the thermal losses, we glued some plates of expanded polystyrene of dimensions 1mm x1 mm and 30 mm thick on the back and side of the sensor.

The choice of expanded polystyrene depends on many reasons, including:

☞ A lightweight insulation: its density is between 10 and 30 kg/m3, that is why it's easy to place.
☞ Good thermal insulation: its thermal conductivity is 0.038 W/m.K.
☞ Affordability.

The insulation properties are presented in the following table:

Table 7: Thermal physical properties of insulation

Physical properties	Symbols	Values
Density ($Kg.m^{-3}$)	P	10 -30
Specific heat (J.Kg1.K1)	Cp	1200-1400
Thermal conductivity ($J.m^{-1}.s^{-1}.K^{-1}$)	Λ	0.032-0,038

The insulation must have high specific heat and low thermal conductivity in order to improve the thermal efficiency of the sensor.

IV.6. Ventilation

The used ventilator is 72x72mm in size. It has three wires to drive the ventilation in both directions including two wires (direction 1: air injection inside the panel) are directly connected to a stabilized power supply which will provide a variable DC voltage to obtain the desired speed and therefore the requested flow rate.

IV.7. The funnel

To properly place the ventilator on the side of the module, a support will be designed. It is trapezoidal in shape and consists of four galvanized steel sheets. The funnel has two bridles: a front bridle on which the ventilator is fixed by screws (countersunk head screw M4), and a rearward bridle which will ensure the assembly with the module. In this face, we made a central hole of 18.5 mm diameter for air injection.

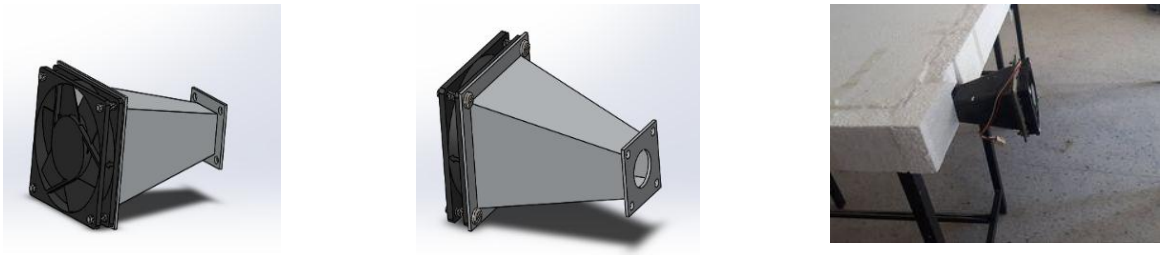

Figure 7: Funnel-ventilator assembly

V. EXPERIMENTAL RESULTS

The objective of this work is to show the influence of different parameters such as the number of fins, solar radiation, and airflow mass rate on the thermal and electrical efficiency of the sensor. The results are presented in the form of graphs developed on Excel and justified by histograms. The experimental measurements are carried out successively in June and July to guarantee the same sunshine and the same temperature. Therefore, Current and voltage measurements as well as input and output temperatures are taken every 30 minutes.

The figure below (Figure 8) presents a simplified diagram of the different components to be used to test the proposed solution.

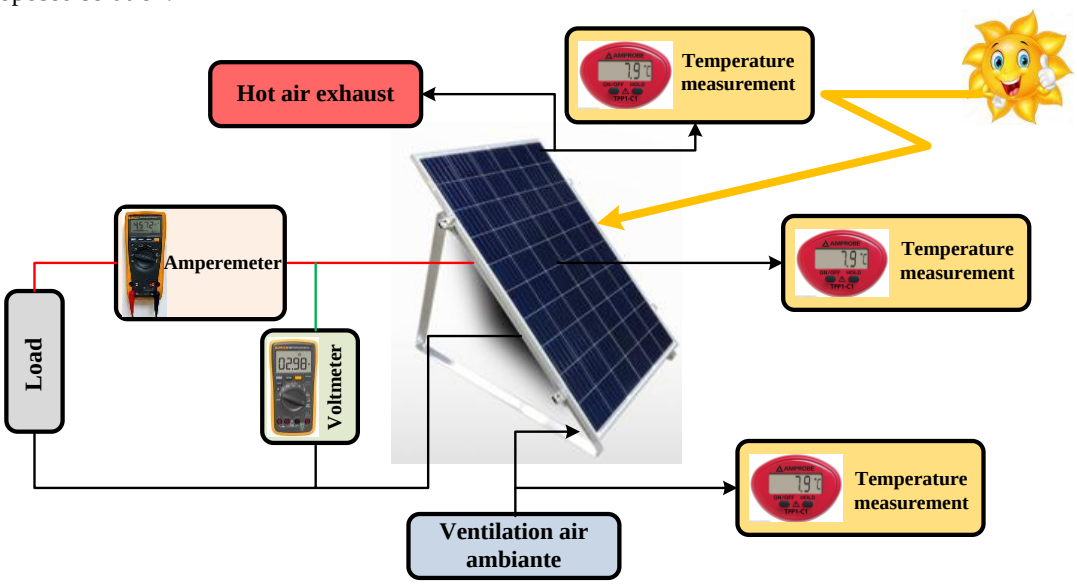

Figure 8. Simplified diagram of the components to be used to validate the proposed solution

The performance of the proposed air PVT sensor is verified by an experimental bench. Experimental results are presented for the following test cases:

- Variation of solar irradiation for an air flow equal to 0.002778 Kg/s.
- Variation of the air flow
- Variation of fins and solar irradiation for an air flow equal to 0.002778 Kg/s
- Variation of fins and solar irradiation for an air flow equal to 0.004167 kg/s

During the experimentation phase, we will determine the electrical gain which is given by expression 6, the thermal balance which is calculated from expression 7 and the thermal gain which is presented by expression 8.

$$\mathbf{Gain_{Electrical}\,\%} = \frac{\mathbf{P_{max-cooling}} - \mathbf{P_{max-without-cooling}}}{\mathbf{P_{max-without-cooling}}} \cdot \mathbf{100} \quad (6)$$

$$\mathbf{Q} = \mathbf{m} \cdot \left(\mathbf{C_{pc}} \cdot \mathbf{T_c} - \mathbf{C_{pf}} \cdot \mathbf{T_f} \right) \quad (7)$$

With :

Q = heat quantity
m = Air mass flow
$\mathbf{C_{pc}}$ = Heat capacity of hot air
$\mathbf{C_{pf}}$ = Heat capacity of cold air
$\mathbf{T_c}$ = Hot air temperature
$\mathbf{T_f}$ = Cold air temperature

$$\mathbf{Gain_{Thermal}\,\% = \frac{Q_{with-fins} - Q_{without-fins}}{Q_{without-fins}} \cdot 100} \quad (8)$$

V.1. Influence of solar irradiation variation on air PVT sensor performance

In this section, we are interested in comparing the electrical and thermal performance of PVT sensor systems with:

- PVT sensor with 4 fins
- PVT sensor with 9 fins

During this experiment, we will determine, for each solar irradiation and each number of fins, the input and output temperatures of the module PVT. Therefore, the reading of current values as well as voltages for different loads is necessary in order to determine the Current-Voltage (I-V) and Power-Voltage (P-V) characteristics of the air PVT sensor.

- Air PVT sensor with 4 fins: Figures 9 show the P-V and I-V characteristics of the air PVT sensor and the PV sensor for different insolation and for a constant air mass flow of 0.002778Kg/s. As a first reading, we notice that the output temperature increases which shows that there is a thermal gain.

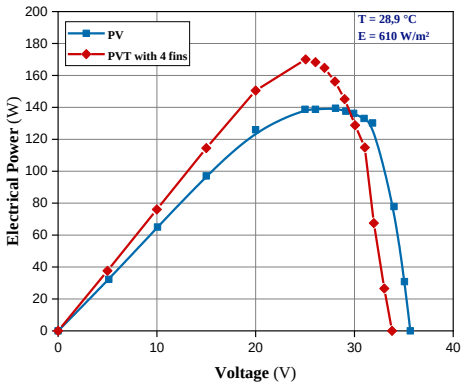

(a)

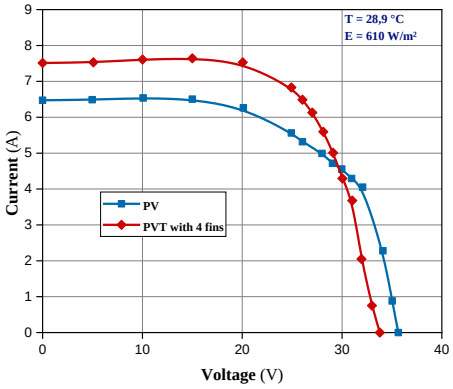

(b)

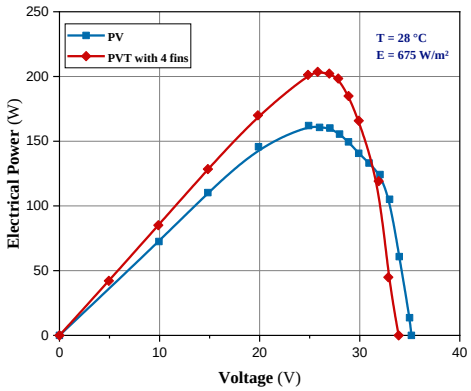

(c)

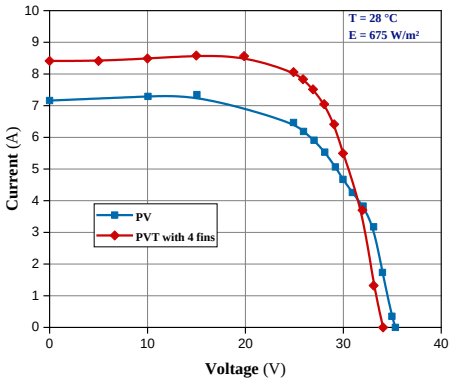

(d)

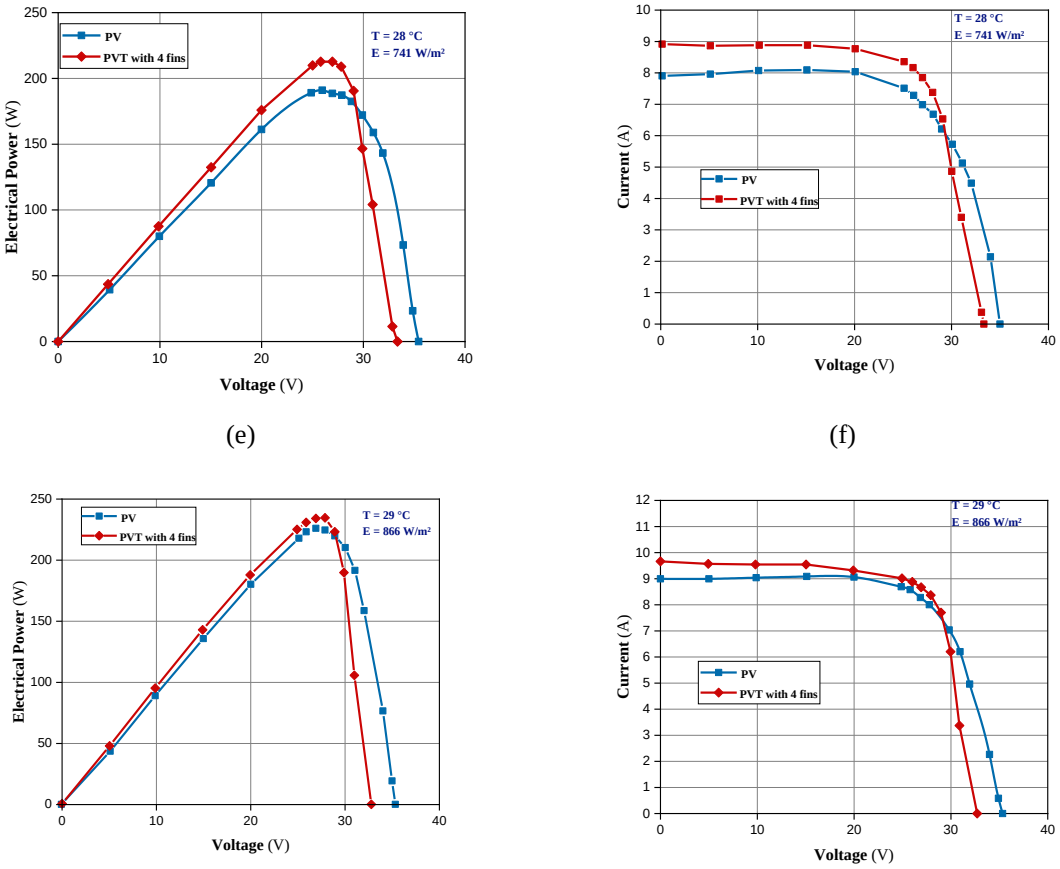

(e) (f)

(g) (h)

Figure 9: P-V and I-V characteristic for an air PVT sensor with 4 fins

The P-V characteristics show that the PVT sensor's MPPT is larger than that of the PV sensor even with increased sunlight, which proves that there is an electrical gain of the proposed system. This gain can reach 24.8% for a temperature of 28°C and sunshine of 675W/m^2.

On the thermal side, we note that a production of a heat quantity (Q) can exceed 55.9 W (for a temperature of 28°C and solar irradiation of 741W/m^2). It is interesting to note that there is no proportionality (whether on the electrical or thermal gain side) between the PV and the PVT sensor when the solar irradiation increases.

Table 8 summarizes the electrical and thermal gains for the different types of solar irradiation.

***Table 8** : Electrical and thermal gains for different levels of solar irradiation (4 fins).*

Solar irradiation (W/m^2)	610	675	741	866
Input temperature (°C)	28,9	28	28	29
Output temperature (°C)	44,9	43,3	48.1	42,3
Electrical gain %	22,14	24,8	12	3,42
Thermal gain W	44,4	42,5	55,9	36,9

So, for 675W/m^2 solar irradiation and a temperature of 28°C:

☞ For an electrical gain of 24.8% and for an installation of 2kWp, there is a production of 4464kWh/year (With a PV sensor the production is 3600 kWh/year)

☞ For a thermal gain of 42.5W and for an installation of 12kWp (42 panels of 275Wp) the thermal power obtained is around of 1785Wh. This quantity can heat an area of 25m^2.

- Air PVT sensor with 9 fins

Figures 10 show the P-V and I-V characteristics of the air PVT sensor and the PV sensor for different insolation and for a constant air mass flow of 0.002778Kg/s. Similarly, we notice that at the output of the air PVT sensor the temperature increases, which shows that there is a thermal gain.

The P-V characteristics reveal that the PVT sensor's MPPT is larger than that of the PV sensor for the first three values of solar irradiation, which proves that there is an electrical gain of the proposed system. While for a sunshine of 866W/m^2 this gain decreases. For the 9 fins, the highest value of the electrical gain is around 12.3% for a temperature of 28°C and solar irradiation of 675W/m^2.

On the thermal side, we note a production of a heat quantity Q does not exceed 32Wh (for the case of a temperature of 28°C and solar irradiation of 741W/m^2).

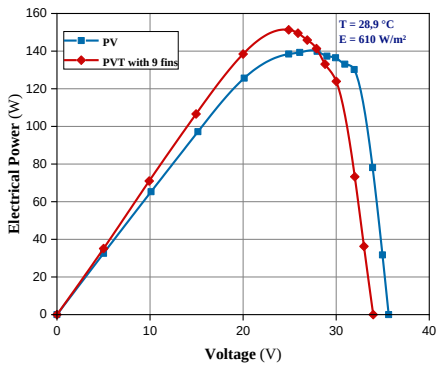

(a)

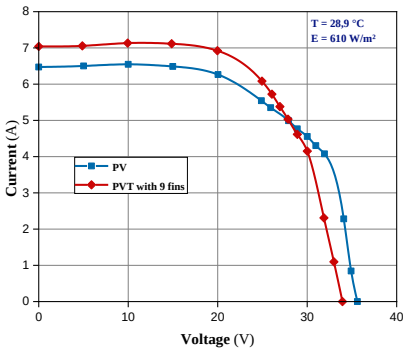

(b)

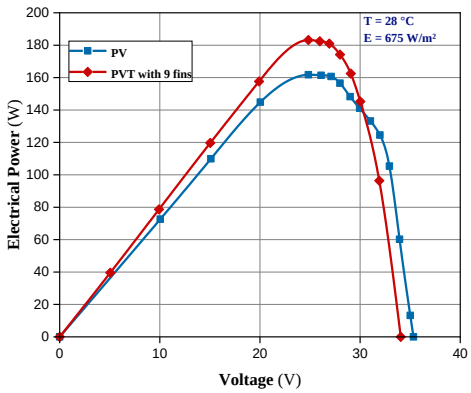

(c)

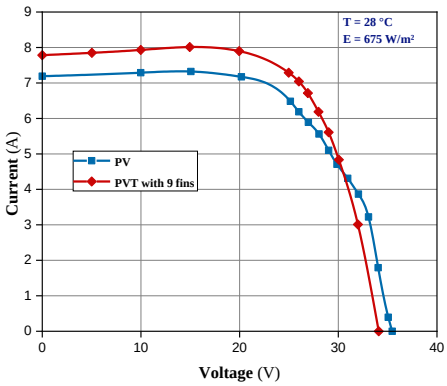

(d)

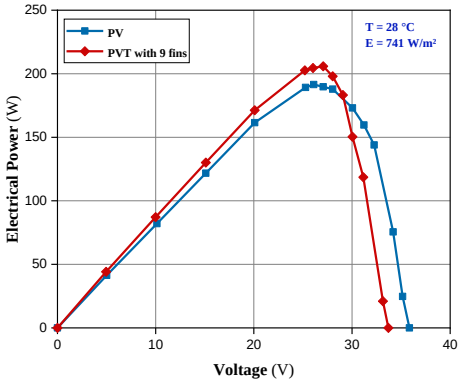

(e)

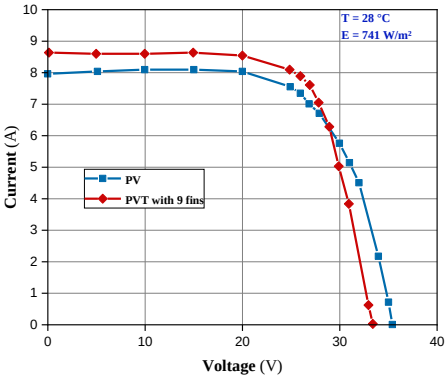

(f)

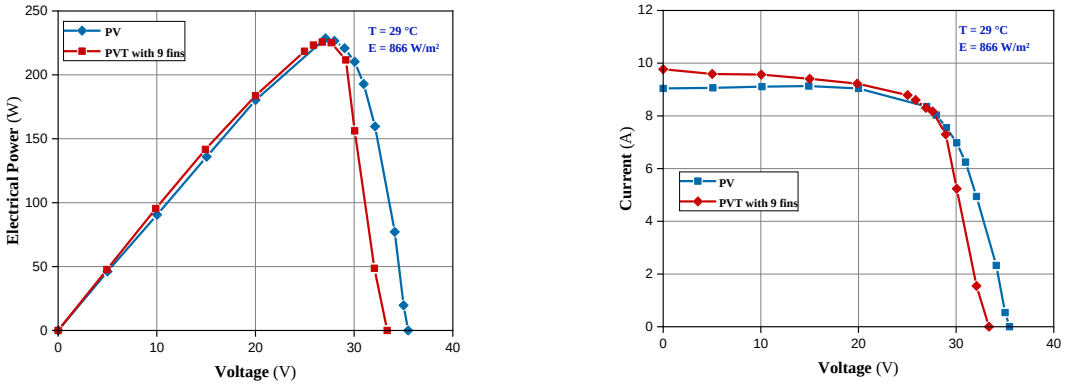

(g) (h)

Figure 10: P-V and I-V characteristic for an air PVT sensor with 9 fins

Table 9 summarizes the electrical and thermal gains for the different levels of sunshine.

Table 9: Electrical and thermal gains for different levels of solar irradiation (4 fins).

Solar irradiation (W/m²)	610	675	741	866
Input temperature (°C)	28,9	28	28	29
Output temperature (°C)	44,9	43,3	48.1	42,3
Electrical gain %	8,21	12,3	7,78	-0,7
Thermal gain (W)	30,5	31,6	51,7	31,4

So, for 675W/m² solar irradiation and a temperature of 28°C:

☞ For an electrical gain of 12.3% and for an installation of 2kWp, there is a production of 4042.8 kWh/year (With a PV sensor the production is 3600 kWh/year)

☞ For a thermal gain of 31.6 W, it requires 56 panels to heat the same area of 25m².

- Comparative study between the PVT air sensor with 4 fins and 9 fins

To make a comparative study between a system with 4 fins and a system with 9 fins, we presented the histogram of the two cases illustrated above.

Figures 11, 12, 13 and 14 represent the air PVT sensor histograms for different solar irradiation values.

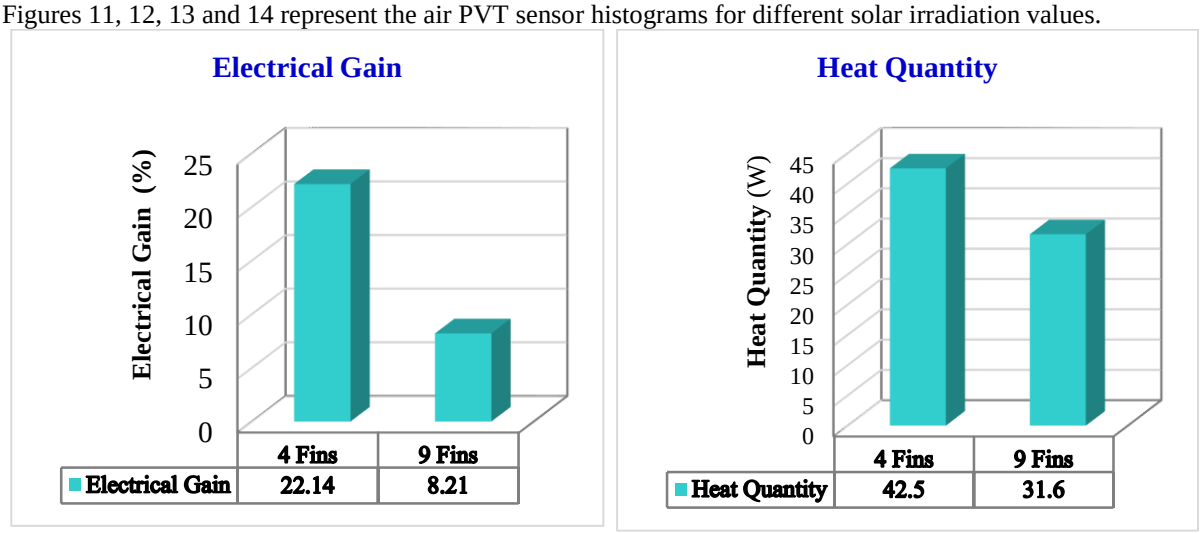

Figure 11: Histograms des gains électrique et thermique d'un capteur PVT pour un ensoleillement de 610W/m²

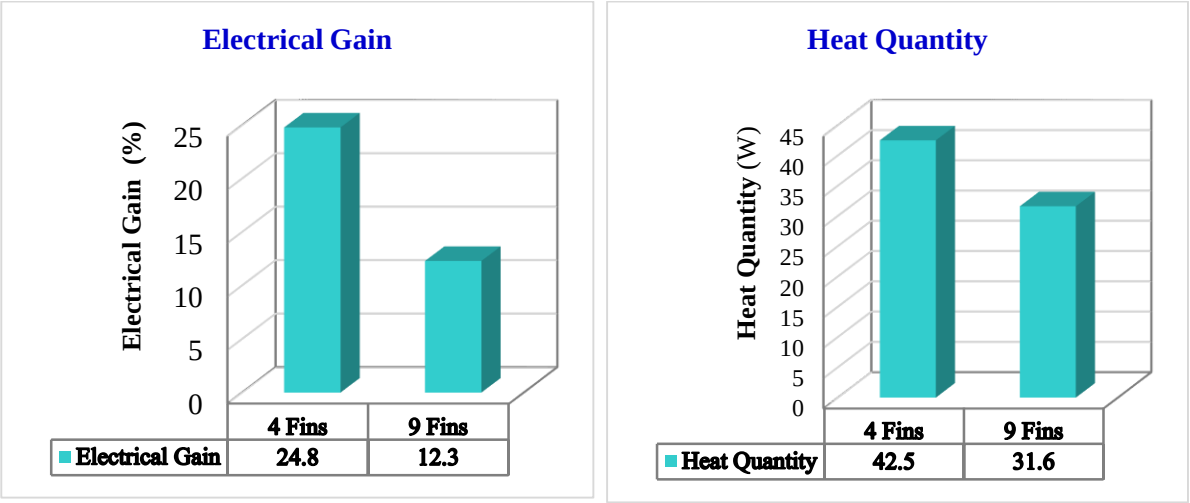

Figure 12 : Histogramme des gains électrique et thermique d'un capteur PVT pour un ensoleillement de 675W/m²

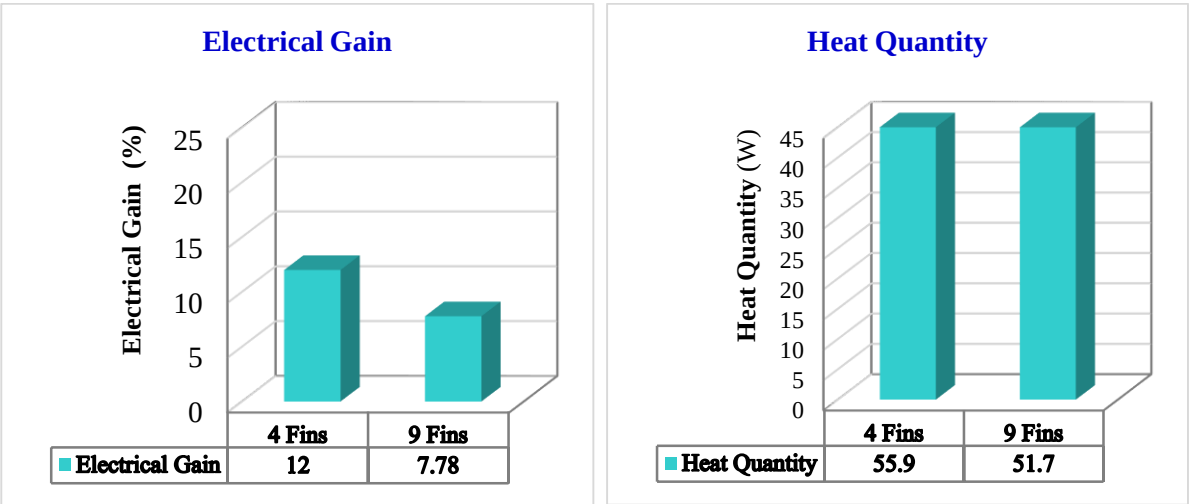

Figure 13: Histogramme des gains électrique et thermique d'un capteur PVT pour un ensoleillement de 741W/m²

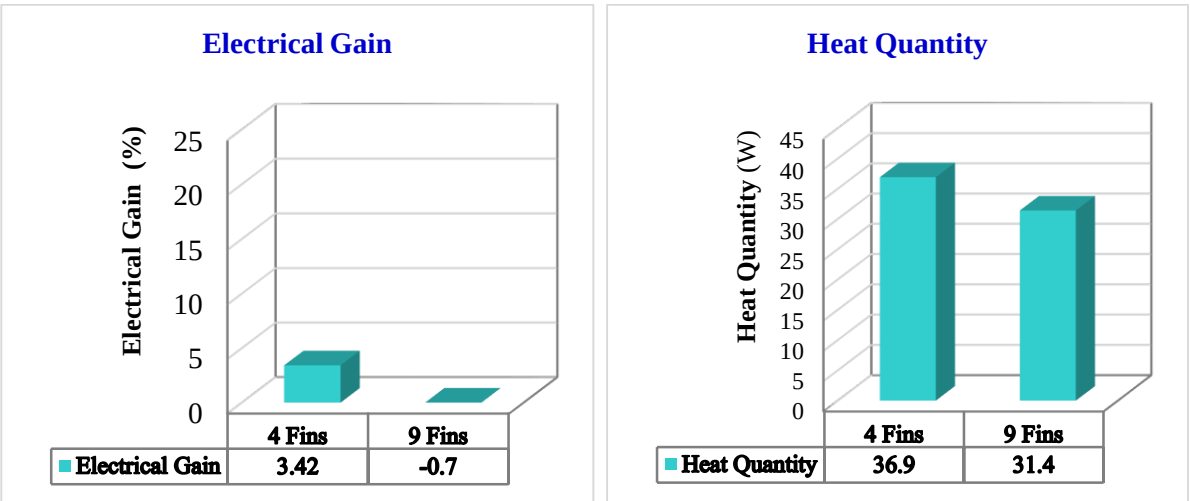

Figure 14: Histogramme des gains électrique et thermique d'un capteur PVT pour un ensoleillement de 866W/m²

The histograms show that for a solar irradiation of 675W/m^2 and with 4 fins we obtained the maximum electrical gain, even the thermal gain is very important. But will this gain be increased if the flow rate is increased?

V.2. Influence of flow rate variation on air PVT sensor performance

To show the influence of the variation of the flow rate on the performance of the air PVT sensor in both cases 4 and 9 fins, we have experimentally determined the Power-Voltage (P-V) characteristics of the PVT panel for two different flow rates.

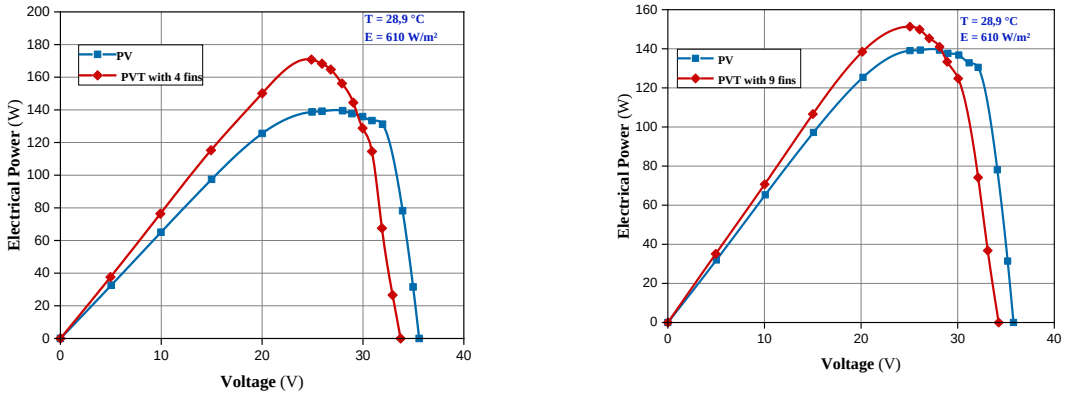

Figure 13 : P-V characteristics of the PVT sensor with 4 and 9 fins for a flow of 0,002778 Kg/s

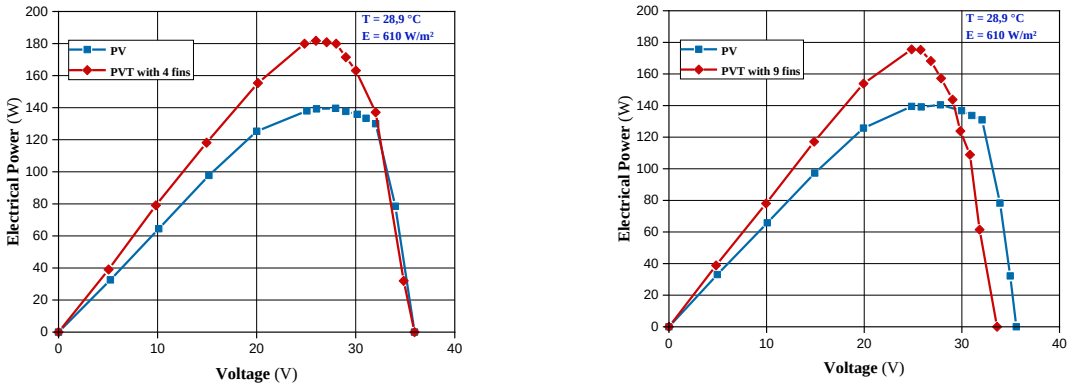

Figure 14 : P-V characteristics of the PVT sensor with 4 and 9 fins for a flow of 0,004167Kg/s

Figures 13 and 14 show that with an increase in flow, both electrical and thermal gain increase. But the performance is always better than with the 4 fins, which shows better electrical efficiency and this performance improves with an increase in flow. But if the number of chicanes is framed between 4 and 9 does the performance improve even more?

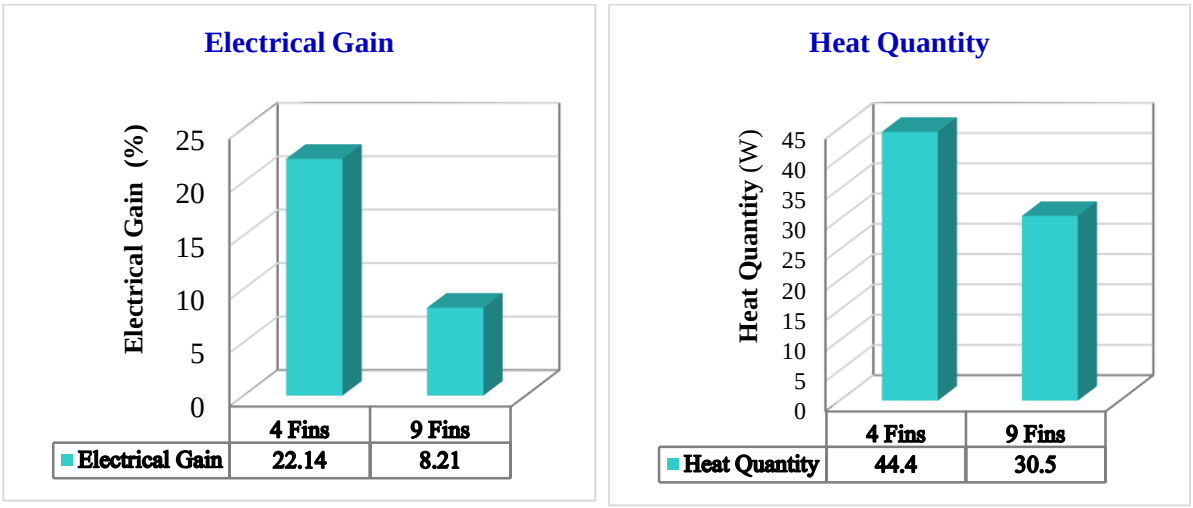

Figure 15 : Histogram with 4 and 9 fins for a flow rate of 0,002778 Kg/s

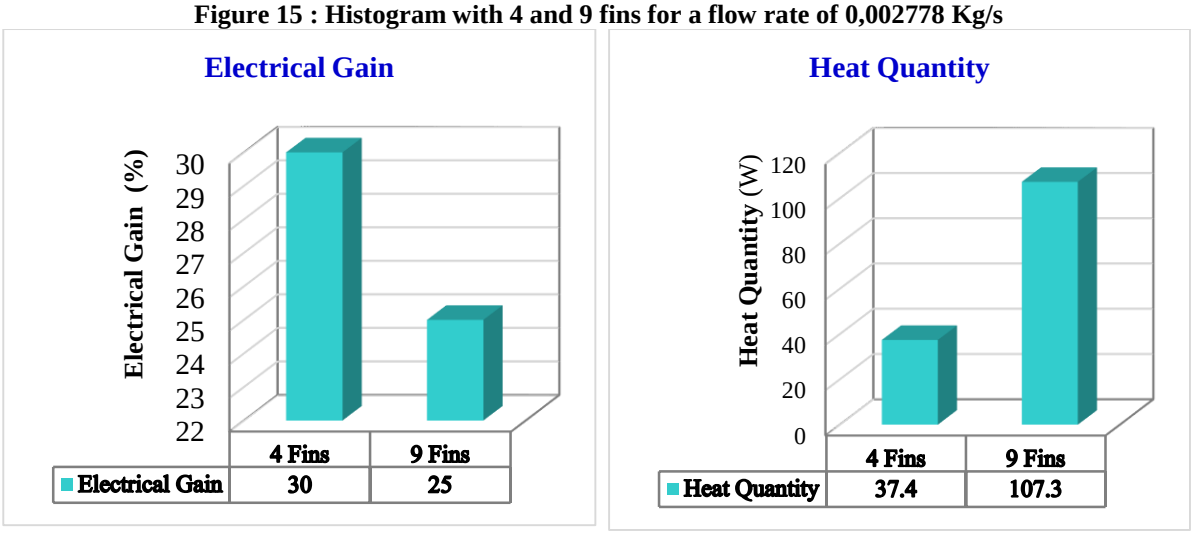

Figure 16 : Histogram with 4 and 9 fins for a flow rate of 0,004167Kg/s

V.3. Influence of fins number variation on air PVT sensor performance at a flow rate of 0.002778 Kg/s

According to the previous study, we have found that it is preferable to optimize the necessary number of baffles to ensure maximum electrical gain. However, an experimental study will be presented to show the effect of the variation in the number of baffles on the Power-Voltage and Current-Voltage characteristics of the air PVT sensor. Therefore, we determined the P-V and I-V characteristics when we have 0 fin, then for 4 fins, then for 6 fins and finally when we have 9 fins. Note that these tests are taken for a temperature of 32°C and for a solar irradiation of 536W/m^2.

Figures 17, (a), (b), (c), (d), (e), (f), (g) and (h) show the PV and IV characteristics for baffles 0, 4, 6 and 9 when the temperature is equal to 32°C, solar irradiation at 536W/m^2 and a constant flow rate of 0.002778 Kg/s. The experimental results show that with 4 fins we obtained the maximum power (MPPT) and consequently the maximum electrical gain is of the order of 21.3%. In addition, with the 4 fins, we were able to produce a thermal energy gain of 23%. Note that the calculated gains (thermal) are by contribution to a PVT system without fins. In addition, when the number of fins is greater than 4, the electrical gain decreases but the thermal gain increases (only for the 6 fins). The case of 9 fins is not recommended since there is a loss of energy for both electrical and thermal cases. Figure 18 and Table 10 provide a general overview of the comparative study of variation in number of fins.

Table 10 : Electrical and thermal gains for different fins

Number of fins	0	4	6	9
Solar irradiation (W/m^2)	536			
Input temperature (°C)	32			
Output temperature (°C)	47,7	51,3	56.3	47,4
Electrical gain %	5,67	21,3	8,96	-5,42

Thermal gain %	0	23	55	-2

This table shows that on the thermal side, the solution with 6 fins is the best, it can provide us a thermal power of 67.7W, then a number of 27 panels (275Wc) is enough to heat an area of 25 m^2. Unfortunately for these types of installations we are primarily interested in electrical gain, that is why we opted for the solution of 4 fins which has an electrical gain of 21.3%. However, we will obtain a production of 4366.8Wh/year instead of 3600Wh/year for a 2 kWp installation.

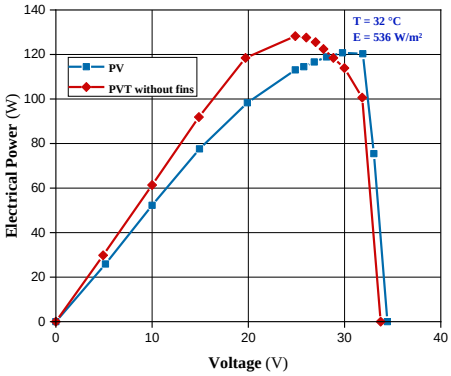

(a)

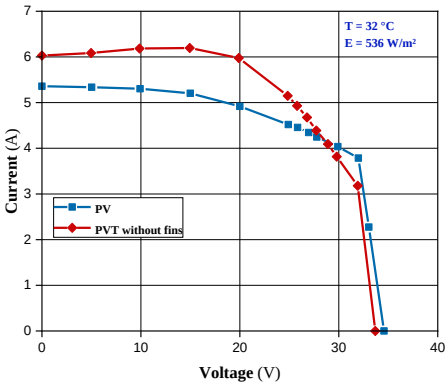

(b)

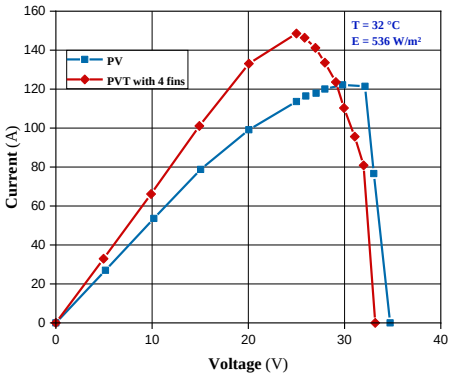

(c)

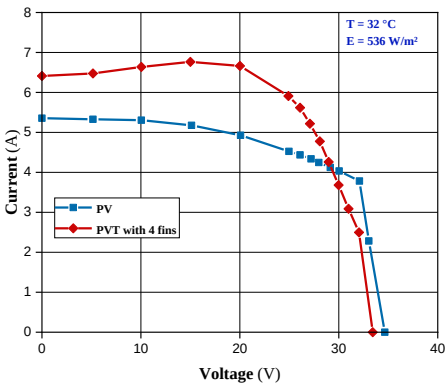

(d)

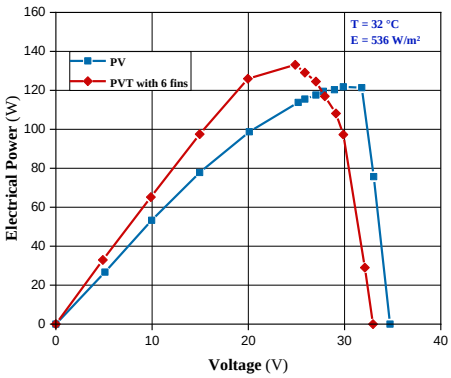

(e)

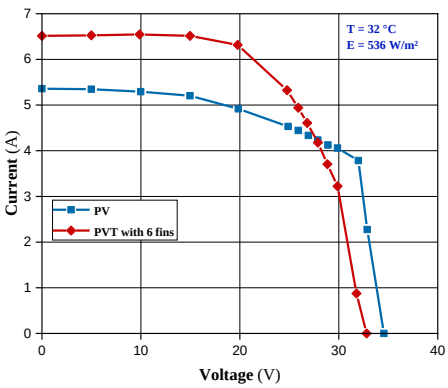

(f)

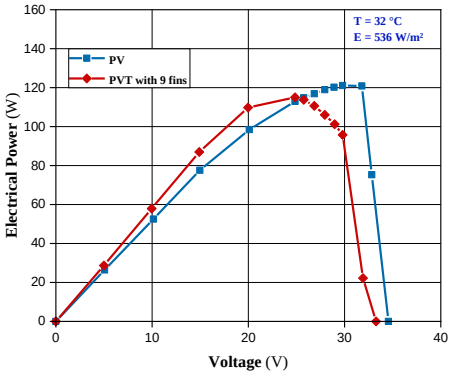

(g)

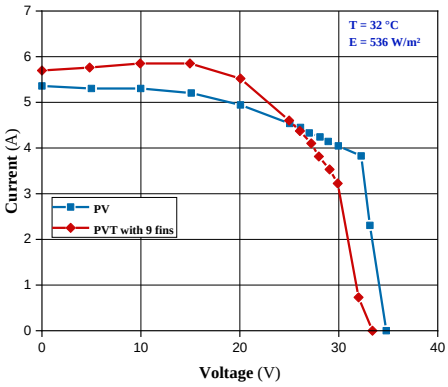

(h)

Figure 17: Characteristics P-V and I-V of an air PVT sensor with several fins for a solar irradiation of 536W/m² and a flow rate of 0.002778Kg/s

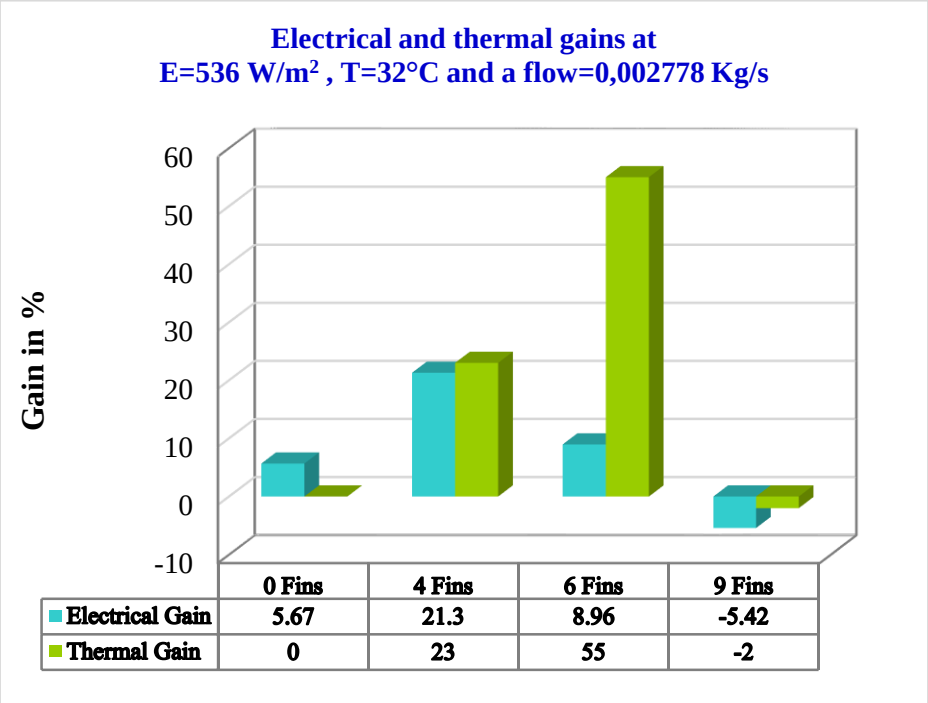

Figure 18 : Electrical and thermal gain histogram for different fins

Variation of sunshine and with a mass flow rate of 0.002778 kg/s

Figures 19 and 20 show the practical characteristics P-V and I-V for two different types of solar irradiation, which are higher than the previous solar irradiation value. These curves always show a higher MPPT than a PV panel without cooling. However, in figure 19 and for a solar irradiation of 623W/m², the PVT air sensor with 4 fins shows a better electrical efficiency which presents an electrical gain of 22%. Moreover, when the solar irradiation increases (figure 20), the electrical efficiency (for 4 fins) decreases and the solution with 6 fins becomes more practical and has the maximum electrical efficiency. On the thermal energy production side, the histograms in figures 21 and 22 show that the PVT air collector with 6 fins always produces more thermal energy. The table 11 summarizes the electrical and thermal gains obtained for different levels of solar irradiation.

***Table 11**: Electrical and thermal gains for different fins*

Numbers of fins	0	4	6	9	0	4	6	9
Solar irradiation (W/m²)	623				700			
Input temperature (°C)	33				33			
Output temperature (°C)	52,4	55	56,5	51,6	53,2	52	60	53,4
Electrical gain %	17,8	22	0,37	5,6	12,22	18	19,35	7
Thermal gain %	0	13,5	21,2	-4	0	-6	33,7	0,88

According to the results found, we note that the number of fins depends primarily on solar irradiation. In our case, if the solar irradiation is less than 700W/m^2, the PVT air sensor with 4 fins then produces the maximum electrical power, while for sunshine greater than 700W/m^2 the solution of 6 fins is the most suitable.

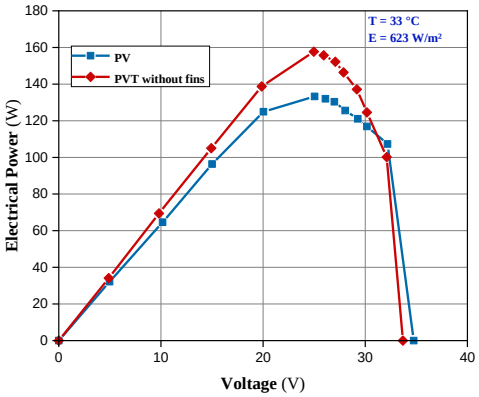

(a)

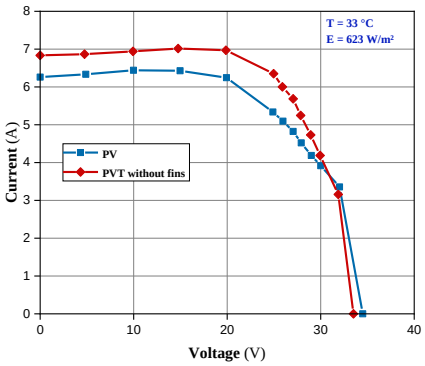

(b)

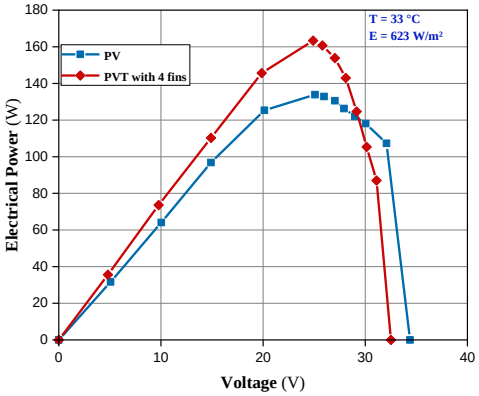

(c)

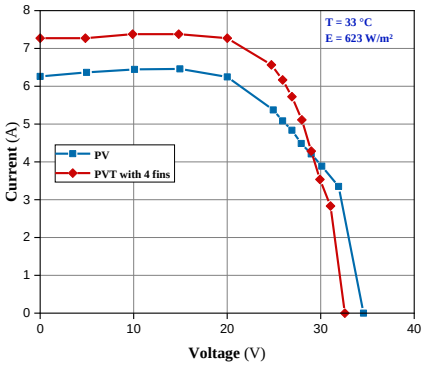

(d)

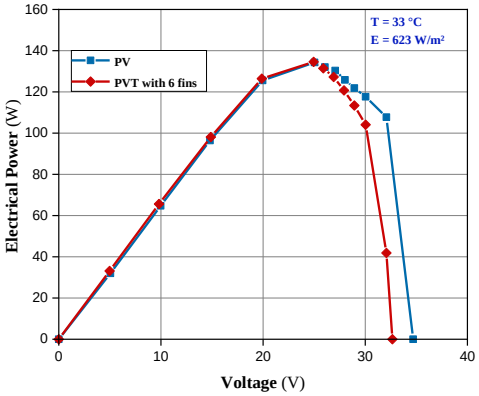

(e)

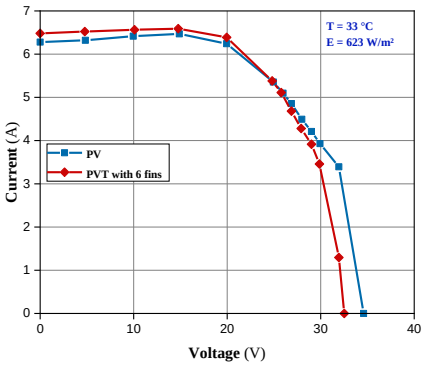

(f)

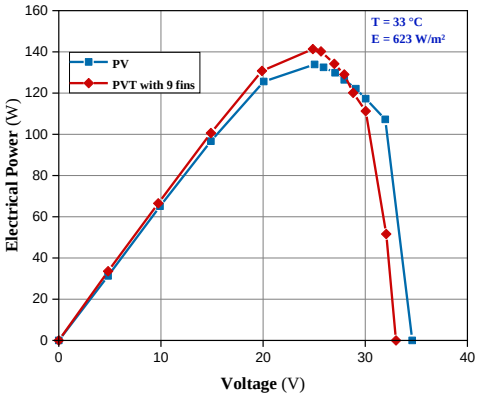

(g)

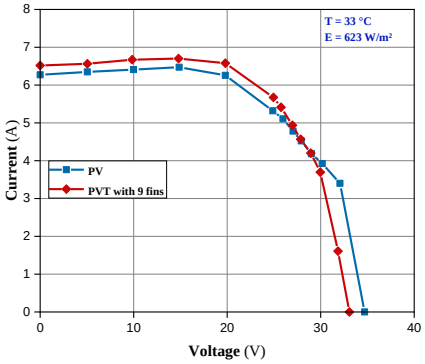

(h)

Figure 19: P-V and I-V characteristics of an air PVT sensor with several fins for a solar radiation of 623W/m² and a flow rate of 0.002778Kg/s

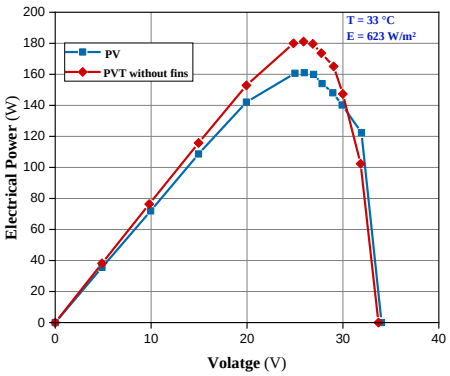

(a)

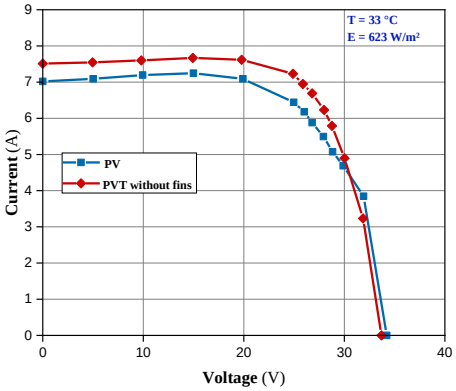

(b)

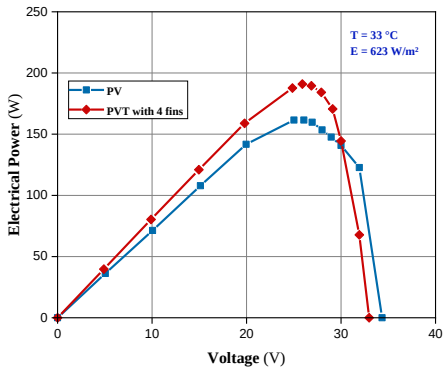

(c)

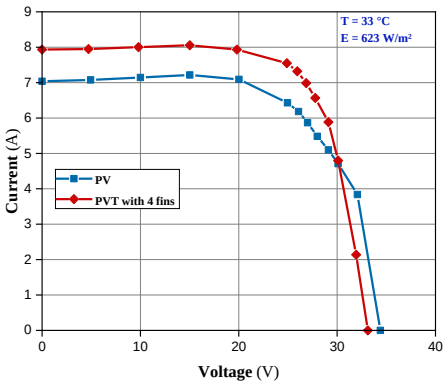

(d)

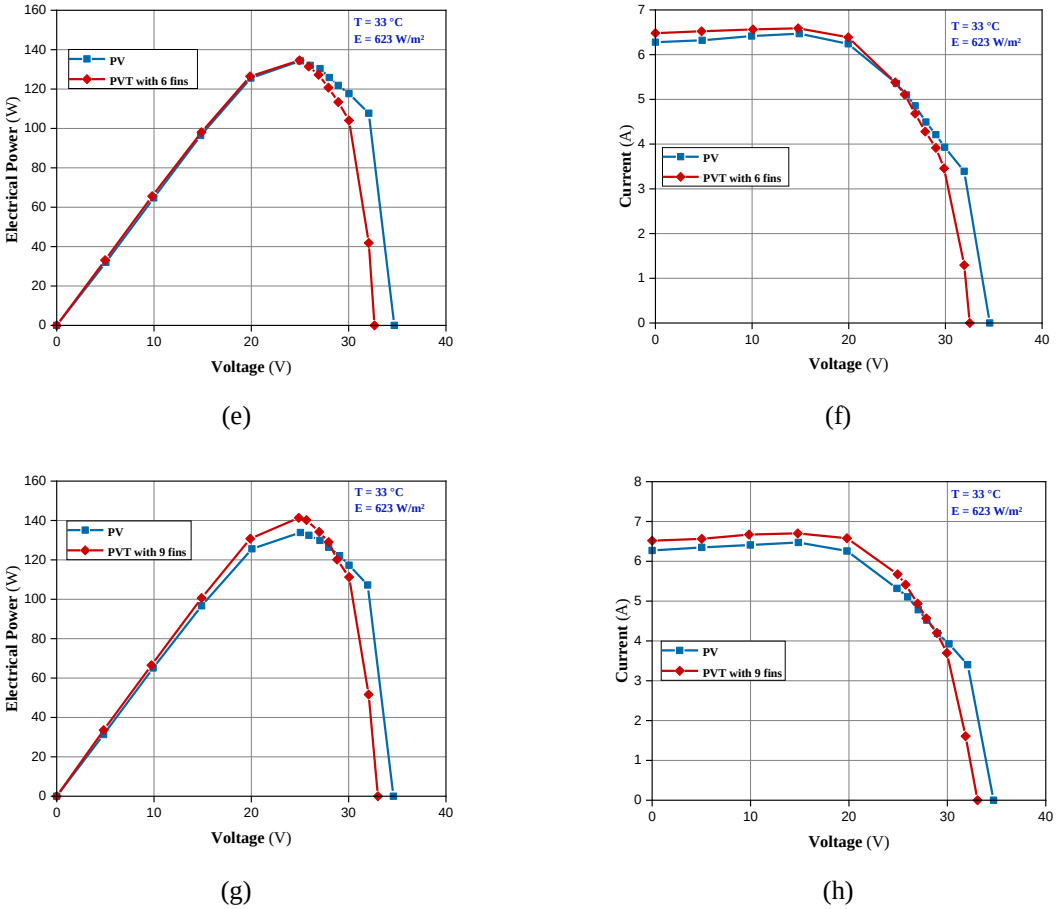

Figure 20: P-V and I-V characteristics of an air PVT sensor with several fins for a solar radiation of 700W/m^2 and a flow rate of 0.002778Kg/s

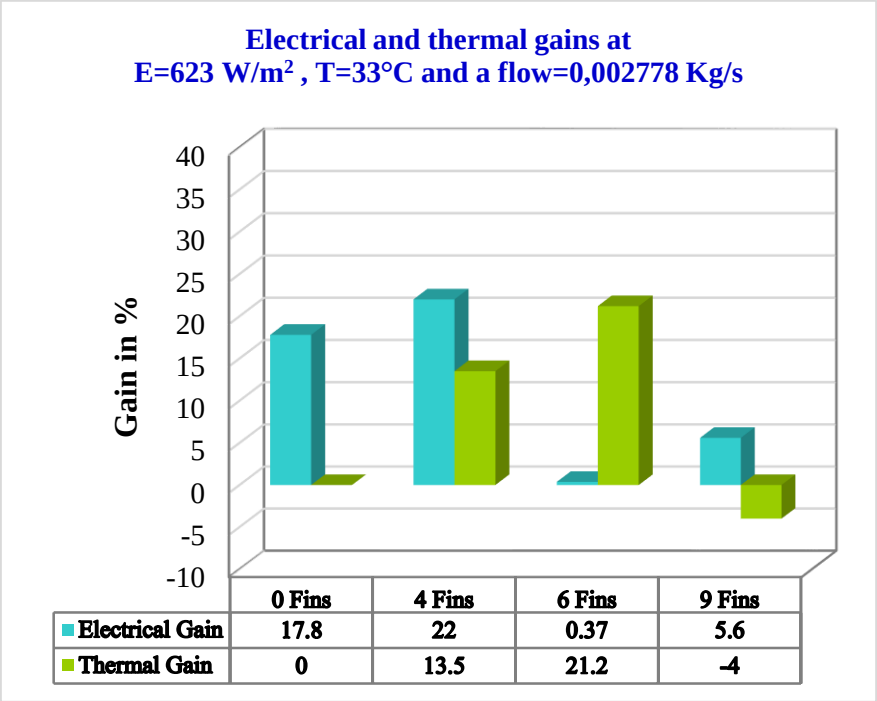

Figure 21: Histogram of electrical and thermal gains for different fins at 623W/m^2 solar irradiation

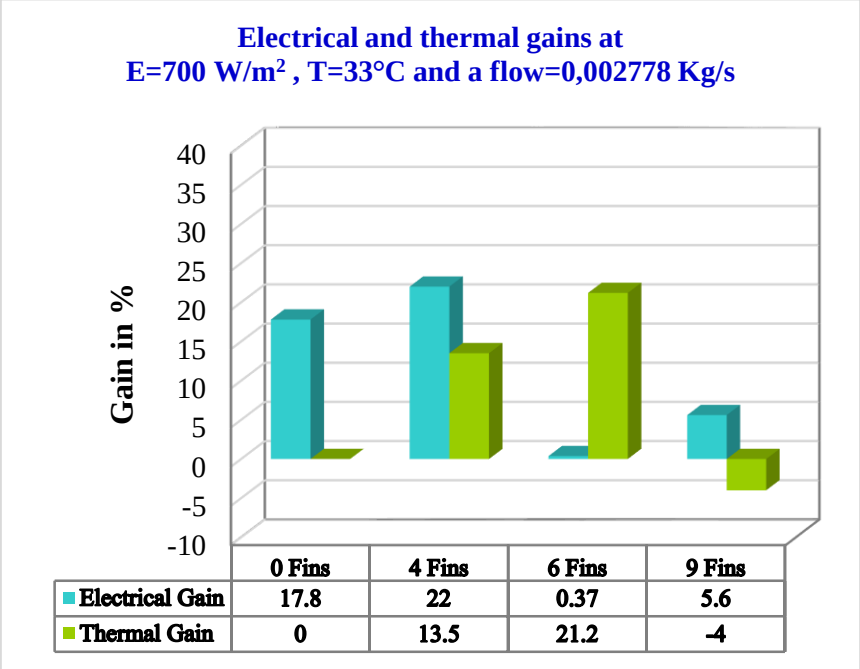

Figure 22: Histogram of electrical and thermal gains for different fins at 700W/m² solar irradiation

V.4. Influence of fins number variation on air PVT sensor performance at a flow rate of 0.004167 Kg/s

In order to determine the influence of the increase in flow rate on the performance of the air PVT sensor in the case where there is a variation in the number of fins, we have experimentally determined the Power-Voltage (P-V) characteristics of the PVT panel for a flow rate of 0,004167 kg/s.

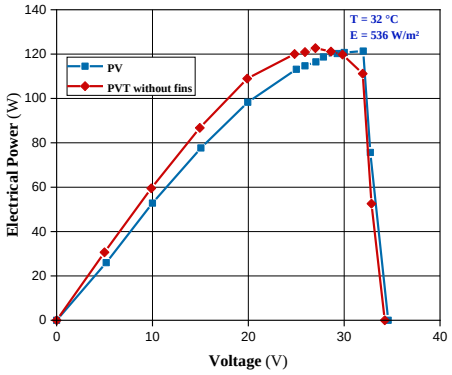

(a)

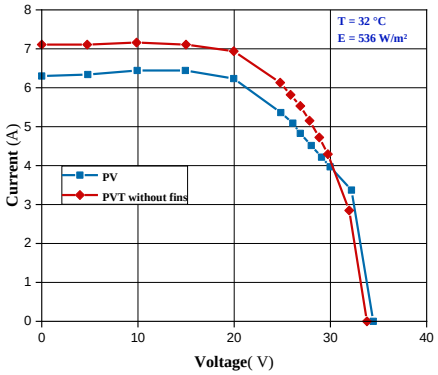

(b)

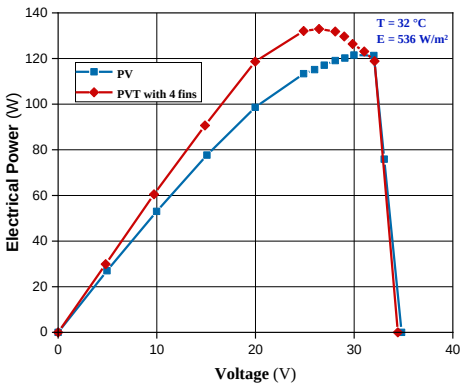

(c)

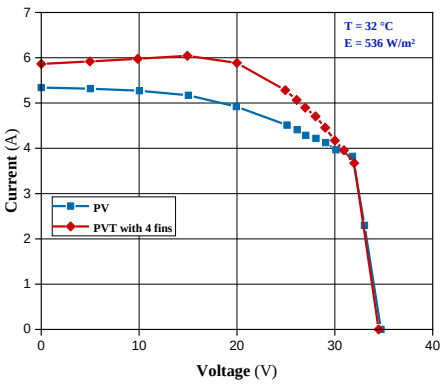

(d)

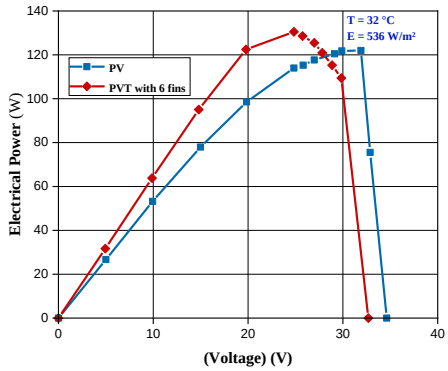

(e)

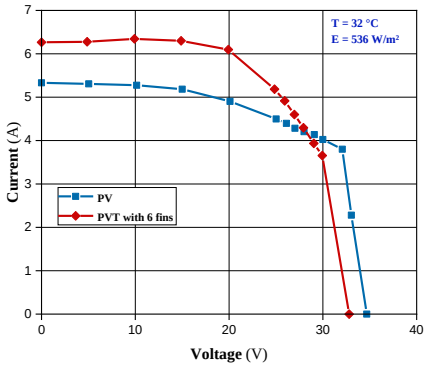

(f)

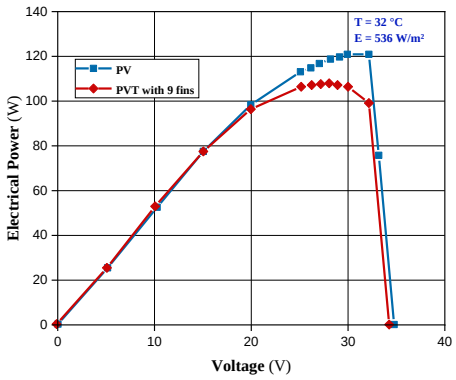

(g)

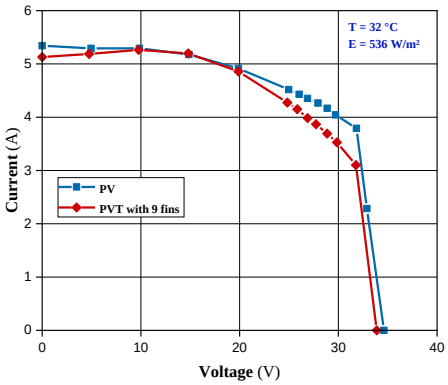

(h)

Figure 23: P-V and I-V characteristics of an air PVT sensor with several fins for a solar radiation of 536W/m² and a flow rate of 0.004167Kg/s

The figures 23, 24 and 25 show that an increase in flow leads to an increase in electrical gain (for different levels of solar irradiation), except in the case where we have installed 9 fins. Indeed, the electrical efficiency is more efficient for the case of the 6 fins. Furthermore, the histograms of figures 26, 27 and 28 illustrate that the maximum thermal efficiency is obtained when we use 6 fins in the air PVT sensor.

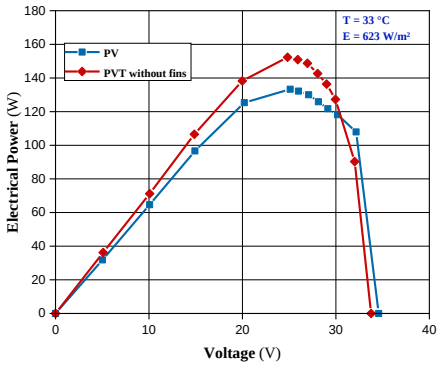

(a)

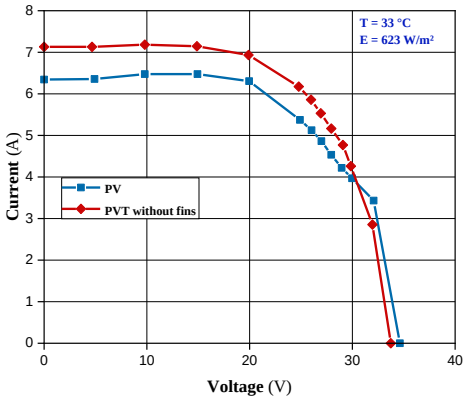

(b)

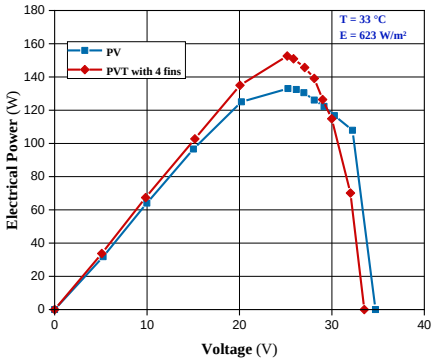

(c)

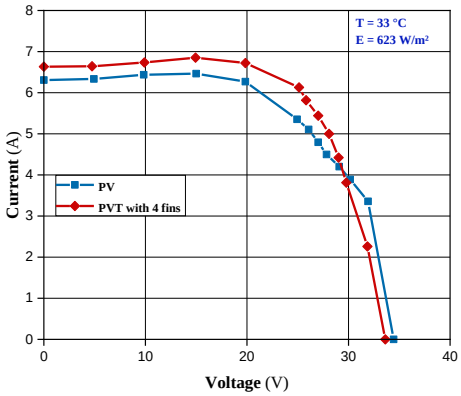

(d)

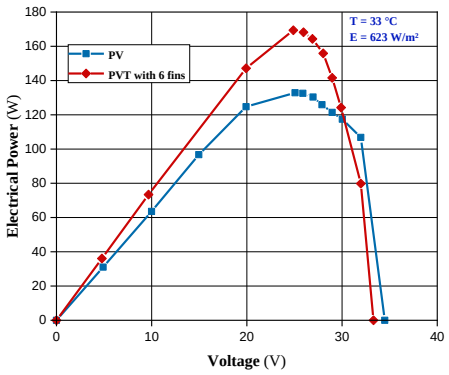

(e)

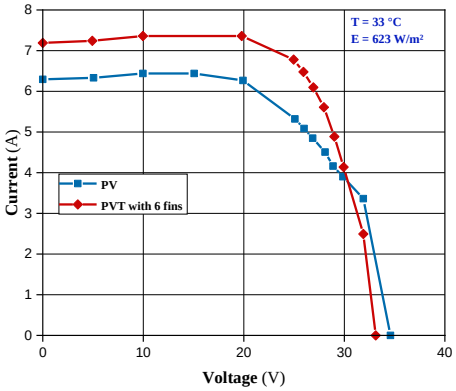

(f)

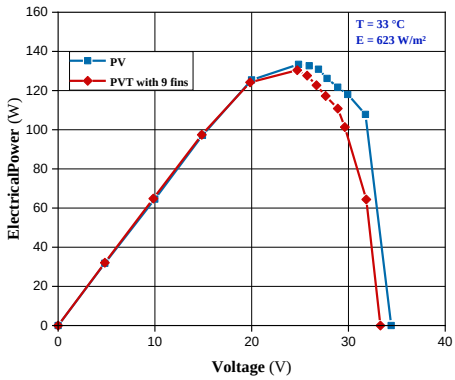

(g)

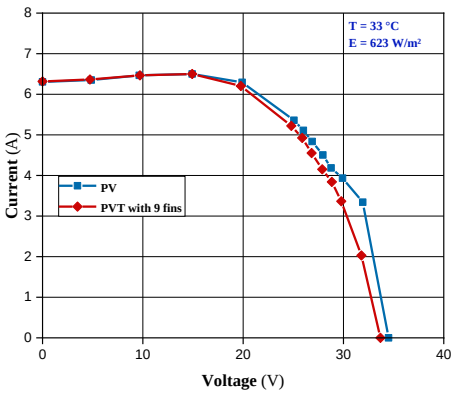

(h)

Figure 24: P-V and I-V characteristics of an air PVT sensor with several fins for a solar radiation of 623W/m² and a flow rate of 0.004167Kg/s

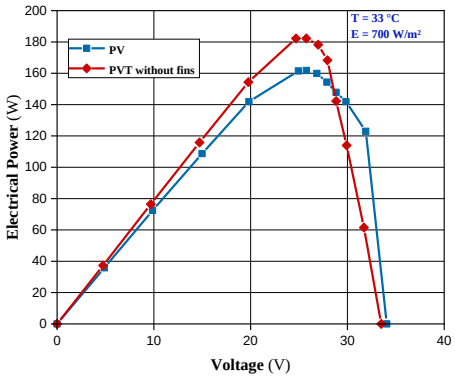
T = 33 °C
E = 700 W/m²
PV
PVT without fins
Electrical Power (W)
Voltage (V)

(a)

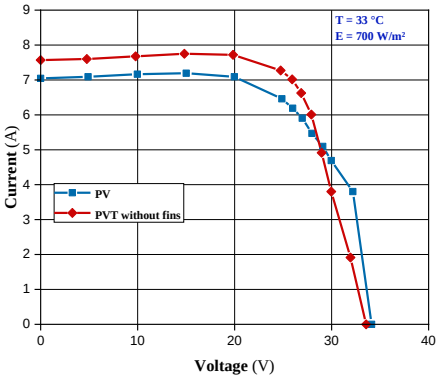
T = 33 °C
E = 700 W/m²
PV
PVT without fins
Current (A)
Voltage (V)

(b)

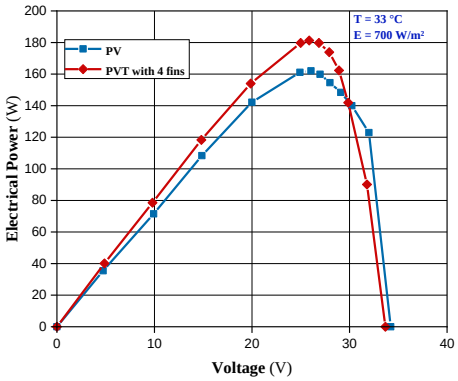
T = 33 °C
E = 700 W/m²
PV
PVT with 4 fins
Electrical Power (W)
Voltage (V)

(c)

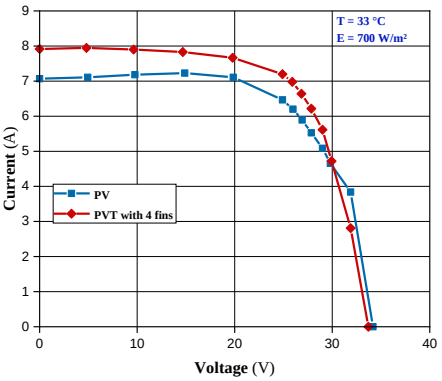
T = 33 °C
E = 700 W/m²
PV
PVT with 4 fins
Current (A)
Voltage (V)

(d)

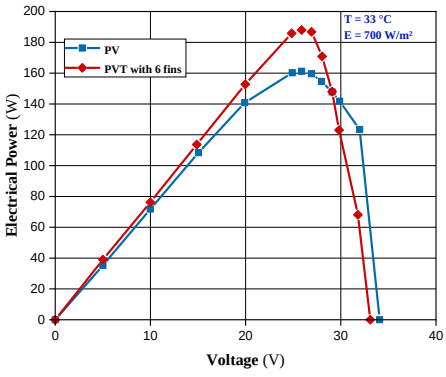
T = 33 °C
E = 700 W/m²
PV
PVT with 6 fins
Electrical Power (W)
Voltage (V)

(e)

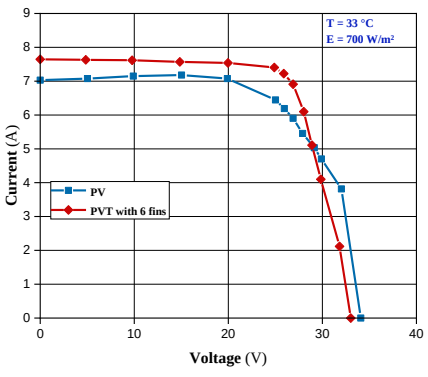
T = 33 °C
E = 700 W/m²
PV
PVT with 6 fins
Current (A)
Voltage (V)

(f)

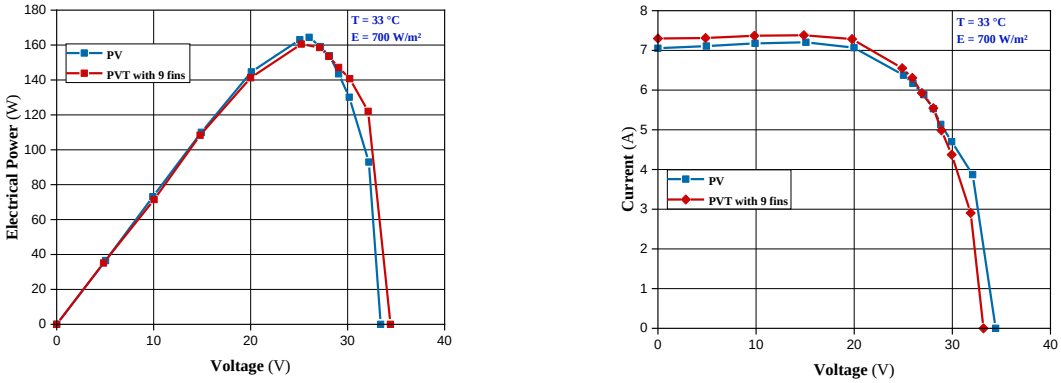

(g) (h)

Figure 25: P-V and I-V characteristics of an air PVT sensor with several fins for a solar radiation of 700W/m^2 and a flow rate of 0.004167Kg/s

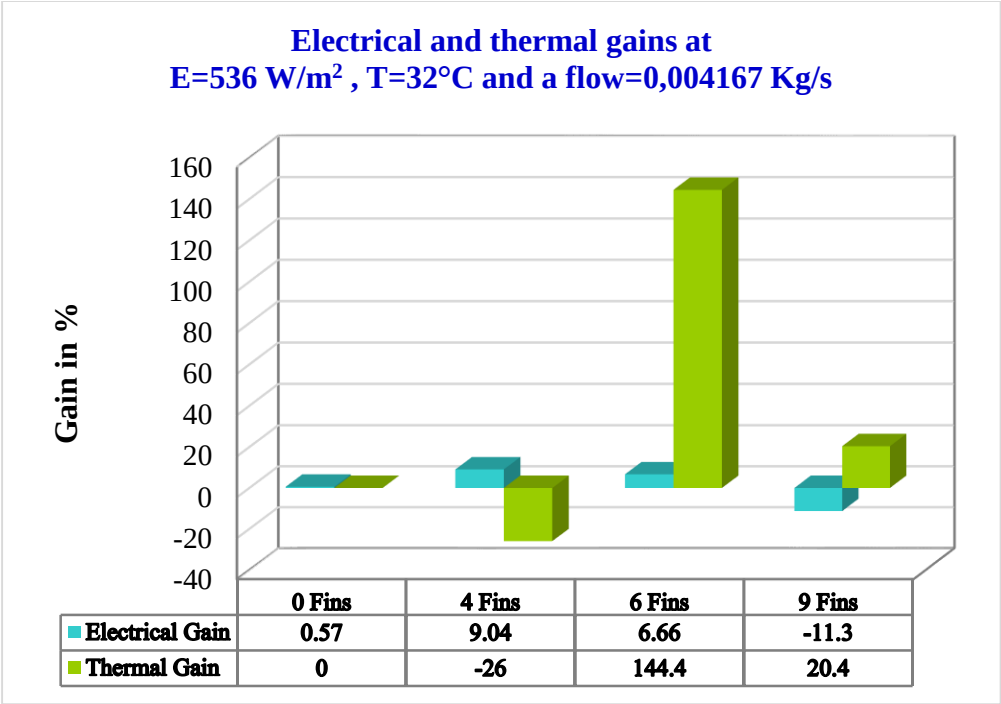

Figure 26: Histogram of electrical and thermal gains for different fins at 536W/m^2 solar radiation

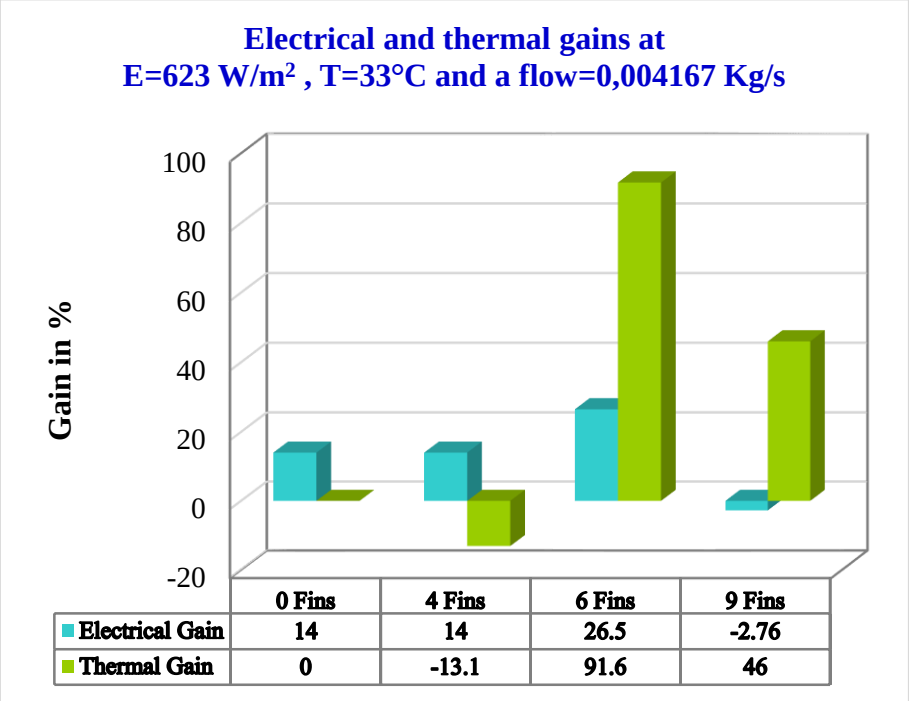

Figure 27: Histogram of electrical and thermal gains for different fins at 623W/m² solar radiation

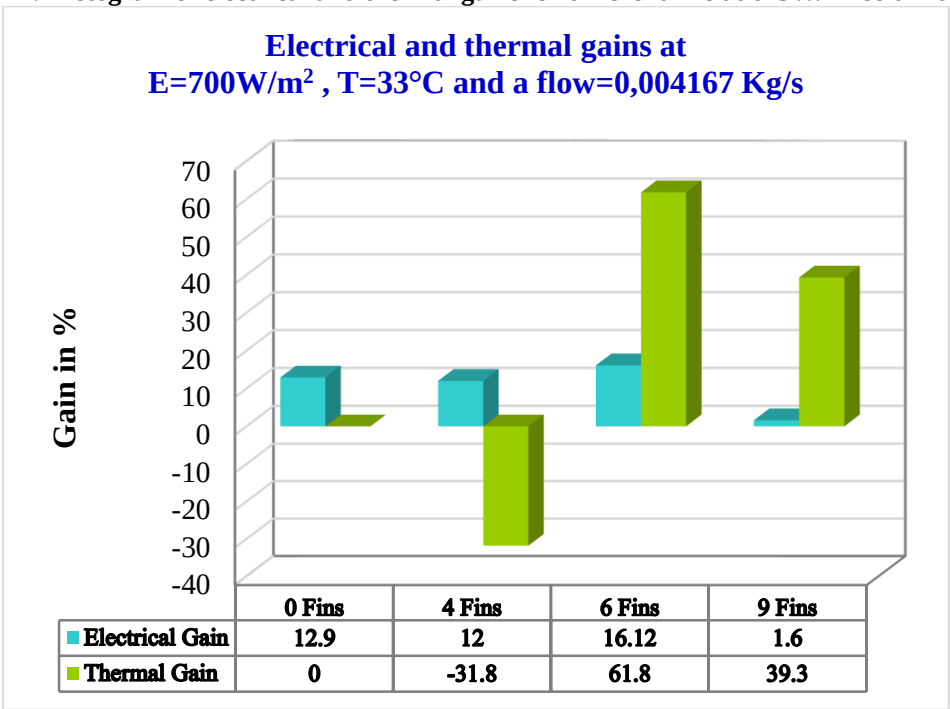

Figure 28: Histogram of electrical and thermal gains for different fins at 700W/m² solar radiation

The table 12 summarizes the gains (electrical and thermal) for 623W/m² and 700W/m² solar radiation.

Table 12 : Electrical and thermal gains for different fins

Numbers of fins	0	4	6	9	0	4	6	9
Solar irradiation (W/m²)	623				700			
Input temperature (°C)	33				33			
Output temperature (°C)	44,5	43	55	49,8	47,8	43,1	57	53,6
Electrical gain %	14	14	26,5	-2,75	12,9	12	16,12	1,6
Thermal gain %	0	-13,1	91,6	46	0	-31,8	61,8	39,3

These results prove that with 6 fins, we have obtained a better performance for both solar radiations.

The table 13 summarizes the founded results. However, we note that for a solar radiation of 623W/m², a flow rate of 0.004167 kg/s and 6 fins, we obtained the best electrical gain (26.5%) as well as thermal gain (91.6%).

Moreover, 3 parameters that will influence these gains, namely the solar radiation, the number of fins and the mass air flow.

Tableau 13 : Electrical and thermal gains for a variation of fins, solar radiation and flow rate

Solar radiations(W/m^2)	623				700			
Fins	4		6		4		6	
Flow rate(.10^{-4}kg/s)	27,78	41,67	27,78	41,67	27,78	41,67	27,78	41,67
Electrical gain %	22	14	0,37	26,5	18	12	19,35	16,12
Thermal gain %	13,5	-13,1	21,2	91,6	-6	-31,8	33 ,7	61,8

VI. CONCLUSION

The objective of this paper is the design and the realization of a thermal photovoltaic sensor with energy recovery in order to improve the performance of the photovoltaic panel. However, the different stages of the realization of the photovoltaic thermal sensor are presented. Afterwards, an experimental study of the PVT air thermal photovoltaic sensor was presented, the aims is to show the performance of this type of sensor and to optimize the number of fins to be installed. Furthermore, according to the founded measurements, the Power-Voltage (P-V) and Current-Voltage (I-V) characteristics are plotted to show the electrical and thermal performance of the proposed solution. After evaluating the influence of some parameters on the electrical and thermal efficiency of the sensor, namely the solar radiation, the number of fins and the mass air flow, we found that the thermal photovoltaic system with 6 fins is the most efficient in solar radiation conditions of 623W/m2, and a flow rate of 0.004167 kg/s.

REFERENCES

[1]. Ahmad FUDHOLI et co, ‘’ Photovoltaic thermal (PVT) air collector with mono facial and bifacial solar cells: a review ‘’ International journal of Power Electronics and Drive System (IJPEDS), Vol. 10, No 4, December 2019, pp. 2021-.

[2]. GHELLAB Amel, ‘’ MODELISATION ET OPTIMISATION DES CAPTEURS SOLAIRES HYBRIDES ‘’, thèse doctorat .

[3]. Feng Shan, Fang Tang, Lei Cao, Guiyin Fang. Comparative simulation analyses on dynamic performances of photovoltaic–thermal solar collectors with different configurations. Energy Conversion and Management 2014; 87:778-786 .

[4]. J.K. Tonui, Y. Tripanagnostopoulos. Air-Cooled PV/T solar collectors with low cost performance improvements. Solar Energy 2007; 81: pp, 498- 511.

[5]. Othman MY. Yatim B. Sopian K, Bakar MNA “Performance analysis of a double –pass photovoltaic/thermal (PV/T) solar collector with CPC and fins” Renewable Energy 2005;30:2005-2017.

[6]. D. Das, P. Kalita, A. Dewan and S. Tanweer, “ Development of a novel thermal model for a PV/T collector and its experimental analysis”, Solar Energy, Volume 188, August 2019, pp 631-643.

[7]. A. Fudholi, M.H. Ruslan, M.Y. Othman, L.C. Haw, S. Mat, A. Zaharim and K. Sopian, “Mathematical Model of Double-Pass Solar Air Collector with Longitudinal Fins”, Recent Advances in Fluid Mechanics, Heat & Mass Transfer and Biology, ISBN: 978-1-61804-065-7, January 2012, pp, 114-120 .